MPPT ALGORITHM FOR PARTIAL SHADING IN FIELD SOLAR POWER STATIONS

by

Çağdaş Altıntaş

Submitted to Graduate School of Natural and Applied Sciences
in Partial Fulfillment of the Requirements
for the Degree of Master of Science in
Electrical and Electronics Engineering

Yeditepe University

2022

MPPT ALGORITHM FOR PARTIAL SHADING IN FIELD SOLAR POWER STATIONS

I hereby declare that this thesis is my own work and that all information in this thesis has been obtained and presented in accordance with academic rules and ethical conduct. I have fully cited and referenced all material and results as required by these rules and conduct, and this thesis study does not contain any plagiarism. If any material used in the thesis requires copyright, the necessary permissions have been obtained. No material from this thesis has been used for the award of another degree.

I accept all kinds of legal liability that may arise in case contrary to these situations.

Name, Last name: Çağdaş Altıntaş

Signature:

ACKNOWLEDGEMENTS

I would like to express my deepest appreciation to my thesis supervisor Prof. Dr. Canbolat Uçak for his continued support, precious thoughts and feedback throughout this dissertation. Also, I am extremely grateful for broadening my academic horizon.

I am also grateful to Prof. Dr. Duygun Erol Barkana and Lecturer Tuğba Haykır Ergin for their guidance and support in my academic life.

Words cannot express my gratitude to my family, who stands by my side and supports me in every decision I make. Their belief in me has kept me motivated and enthusiastic throughout this thesis.

ABSTRACT

MPPT ALGORITHM FOR PARTIAL SHADING IN FIELD SOLAR POWER STATIONS

With the increasing effects of global warming, the transition to renewable energy sources has accelerated in recent years. Solar energy has become more affordable and efficient due to technological improvement. In order to obtain maximum efficiency from PV systems, PV panels should operate at the maximum power point (MPP). Maximum power point tracking (MPPT) algorithms have been developed to achieve maximum power output from PV systems by tracking MPP under different environmental conditions. The proposed method is based on the perturb and observe (P&O) approach. Although the P&O technique can locate the maximum power point in uniform radiation, it is not able to track the global maximum power point in partial shading conditions (PSC). Therefore, the P&O method is combined with an effective global search mechanism to ensure MPP tracking. The global search part of the presented method determines the positions of potential local maximum power points and measures the corresponding power values to these peak points. Then, the highest of these measured powers is chosen as the new operating point of the panel. Thus, the suggested technique is able to obtain the maximum power from the PV panel by tracking the MPP under PSC. Consequently, the proposed algorithm performs effectively in different environmental conditions. MATLAB/Simulink software was used to analyze the tracking performance of the algorithm. The proposed method has been evaluated in heavily and lightly partial shadowing situations, which change dynamically to reflect real-world conditions. The presented algorithm is compared with the simulated annealing algorithm, one of the popular MPPT algorithms in the literature. The simulation result indicates that the tracking efficiency of the presented method is 98.36% to 90.63% higher than the simulated annealing method in the severely shading condition. Similarly, the proposed method tracked the ideal power by 98.38%, while the simulated annealing method remained at 93.53% in the lightly partial shading condition.

ÖZET

GÜNEŞ ENERJISI SANTRALLERINDE KISMI GÖLGELENME İÇIN MPPT ALGORITMASI

Maksimum Son yıllarda küresel ısınmanın etkilerinin artmasıyla birlikte yenilenebilir enerji kaynaklarına geçiş hız kazanmıştır. Güneş enerjisi, teknolojik gelişmeler sonucunda daha uygun fiyatlı ve verimli hale gelmiştir. PV sistemlerinden maksimum verim alabilmek için PV panellerin maksimum güç noktasında (MGN) çalışması gerekir. Maksimum güç noktası takibi (MGNT) algoritmaları, farklı çevre koşullarında MGN'yi izleyerek PV sistemlerden maksimum güç elde etmek için geliştirilmiştir. Önerilen yöntemi değiştir ve gözle (D&G) yöntemine dayanmaktadır. P&O yöntemi, düzgün ışımada maksimum güç noktasını bulabilmesine rağmen, kısmi gölgeleme durumlarında (KGD) global maksimum güç noktasını izleyemez. Bu nedenle, D&G yöntemi, MPP takibini sağlamak için etkili bir global arama mekanizması ile birleştirilmiştir. Sunulan yöntemin global arama kısmı, potansiyel yerel maksimum güç noktalarının konumlarını belirler ve bu tepe noktalarına karşılık gelen güç değerlerini ölçer. Daha sonra ölçülen bu güçlerin en yüksek olanı panelin yeni çalışma noktası olarak seçilir. Böylece önerilen teknik, MPP'yi KGD altında izleyerek PV panelden maksimum gücü elde edebilmektedir. Sonuç olarak, önerilen algoritma farklı çevresel koşullarda etkin bir şekilde çalışır. Algoritmanın izleme performansını analiz etmek için MATLAB/Simulink yazılımı kullanılmıştır. Önerilen yöntem, gerçek dünya koşullarını yansıtmak için dinamik olarak değişen yoğun ve hafif kısmi gölgeleme durumlarında değerlendirilmiştir. Sunulan algoritma, literatürdeki popüler MPPT algoritmalarından biri olan simüle edilmiş tavlama algoritması ile karşılaştırılmıştır. Simülasyon sonucu, sunulan yöntemin izleme verimliliğinin, şiddetli gölgeleme durumunda benzetilmiş tavlama yönteminden %98.36'ya %90.63 daha yüksek olduğunu göstermektedir. Benzer şekilde, önerilen yöntem hafif kısmi gölgeleme durumunda ideal gücü %98,38 takip ederken, benzetilmiş tavlama yöntemi %93,53'te kalmıştır.

TABLE OF CONTENTS

LIST OF FIGURES

LIST OF TABLES

LIST OF SYMBOLS/ABBREVIATIONS

D	Duty cycle
I_{SC}	Short-circuit current
V_{MPP}	Voltage of maximum power point
V_{OC}	Open-circuit voltage
V_{pv}	Voltage of the photovoltaic panel

CEC	California energy commission
DSP	Digital signal processing
FF	Fill factor
FOCV	Fractional open circuit voltage
GMPP	Global maximum power point
GWO	Grey wolf optimization
IC	Incremental conductance
LMPP	Local maximum power point
MPP	Maximum power point
MPPT	Maximum power point tracking
P&O	Perturb and observe
PSO	Particle swarm optimization
PV	Photovoltaic
SA	Simulated annealing

1. INTRODUCTION

Renewable energy sources play a crucial role due to ecological issues and rising energy demand in today's world. Over the past decade, solar energy systems have attracted the most attention out of all the available renewable energy sources. Also, it is predicted that the share of renewable energy among electricity generation methods will rise over the next few decades [1,2].

Solar energy is converted into electrical energy with photovoltaic (PV) cells. The amount of electricity the PV system can produce depends on irradiance and temperature. These environmental factors impact the PV system's nonlinear current-voltage (I-V) and power-voltage (P-V) characteristics, making it challenging to find the optimal operating point corresponding to the maximum power. Another critical factor affecting the PV characteristic is partial shading on the PV panel. Partial shadowing, which can be caused by moving clouds, buildings, or surrounding objects, not only reduces the power output of the PV system but can also damage the PV panel. Bypass diodes are utilized in this mismatch condition to increase the power output of the panel and prevent the panel from being damaged by hot spots. However, the P-V curve may have multiple peaks because of bypass diodes during the partial shading. Therefore, maximum power point tracking (MPPT) in PV systems is challenging and necessary.

Maximum power point tracking algorithms are a critical part of the PV systems. In order to reach the maximum power the system can produce, the MPPT algorithm must work effectively. Although MPPT algorithms generally work well in uniform irradiance, they may get stuck at the local maximum power point in non-uniform irradiance situations, causing power loss. There are many examples in the literature of scanning the entire voltage range and randomly searching the voltage of the PV system to find the global maximum power point (GMPP). Despite the fact that voltage scans can detect GMPP, they reduce the power output of PV systems. Therefore, it is not feasible to implement voltage scans or random searches in high power PV systems.

This present thesis aims to develop a simple and applicable algorithm that can track the maximum power point under partial shading conditions. The power loss in searching GMPP is minimized in the proposed technique by limiting the search to potential LMPPs.

1.1. LITERATURE REVIEW

1.1.1. Conventional Methods

MPPT is required to maximize the power extracted from PV systems. Therefore, in literature, many MPPT techniques are developed for tracking the maximum power point of PV arrays. References [3] and [4] compare the maximum power point tracking techniques. The techniques differ in performance, complexity, data needed, the number of iterations, equipment used, price, and other factors. These techniques, including some intelligent methods, vary from simple to the most complex. Conventional solutions such as perturb and observe (P&O) technique, incremental conductance (IC) technique, fractional short circuit current technique and fractional open-circuit voltage technique are simple and commonly used in practice. In the P&O method, mostly voltage and current are sensed, and the power of the PV array is calculated. The change in power is observed and compared to its previous value by perturbing voltage or current. If the new power is higher than the previous value, the perturbation process is continued in the same path until no change of power is achieved. Thus, the maximum power point (MPP) and corresponding voltage are detected.

In most cases, two sensors that measure voltage and current are needed to calculate the power of PV array, and however, in some applications, only a voltage sensor may be required based on the power converter design. Unlike the P&O algorithm, the incremental conductance method uses the slope of the Power-Voltage characteristic curve. The slope of this curve is zero at MPP, negative on the right side, and positive on the left side of MPP. The incremental conductance ($\Delta I/\Delta V$) is compared to the instantaneous conductance (I/V) to track MPP. Two sensors are required for the IC method. The IC method is suitable for microcontrollers [3].

Another conventional method is fractional open-circuit voltage (FOCV). This approach is based on the relationship between voltage of maximum power point and open-circuit voltage (V_{OC}). Although the constant (k_{OC}) is calculated according to this proportion, it may be recalculated in case of temperature and irradiation change. However, The open-circuit voltage must be measured in order to update k_{OC}, which results in power loss. In addition, this method cannot find the optimum power point in partial shading conditions.

The open-circuit voltage technique is straightforward and cost-friendly to implement because it does not need a microcontroller. Nevertheless, the inadequacy of the partial shading conditions and the power loss while updating the k constant are the negative aspects of the open voltage technique. The fractional short circuit current (FSCC) method calculates a constant similar to the FOCV but measures the short circuit current (I_{SC}) instead of the voltage of the PV array. A switch is installed to the PV array to measure the short circuit current with the current sensor. Hence, the amount of the component and cost of the system increases considerably. The majority of FSCC-based PV systems in the literature use DSP [3].

The P&O algorithm is widely utilized because of its simplicity [3]. It can perform well without needing any knowledge about PV arrays. Thus, it applies to any PV array. However, this algorithm's major drawbacks are power oscillations around MPP and inaccurate MPP detection under rapidly changing atmospheric conditions. In the P&O algorithm, the current and voltage of the PV array are determined, and the corresponding power is computed. By perturbing the voltage or the current of the PV array, the power value is changed, and new calculated power is compared with the prior for the decision. This process is constantly repeated. This repeating process causes power oscillations about the MPP, resulting in power loss [3–6]. Multiple local maximum power points may occur in changing weather conditions or shadow situations. The P&O technique can get stuck in LMPP and cannot escape from that position [7]. To overcome this problem, variable voltage or current perturbation sizes are used in some studies called adaptive P&O algorithms. In steady-state, oscillation can be diminished by changing the perturbation amount. In addition, a good initial starting point is predicted to reach the MPP faster [8–11]. Furthermore, the P&O algorithm is combined with intelligent algorithms aimed at hybrid algorithms to overcome these difficulties [7,12].

P&O method is elemental of the traditional MPPTs and has adequate convergence in uniform shading conditions. However, the algorithm has two serious shortcomings, oscillations in the vicinity of MPP and loss of tracking direction in a rapid change in irradiance [13]. Various methods have been suggested in the literature to overcome these issues [13–17]. In [14], a specific system that analyzes three signs of slope in sequential recognizes the oscillation and decreases the perturbation size. Three various irradiance levels are determined by evaluating the value of the normalized power change. Therefore, perturbation size may adjust between 0.5 percent V_{OC} and 2 percent V_{OC} according to the irradiation level. Although the oscillation decreases when the perturbation size is small-scale, the tracking direction may be lost in case of irradiance changes rapidly. A flag is used to prevent this issue. In the beginning, the flag is set low until the oscillation is recognized, turning it to high. The position of the flag changes by comparing the normalized power change values with specified thresholds. The initial voltage limits have been established. The limits are modified by adding a 5 percent margin of V_{OC} to V_{MPP}. As a result of this margin, the MPPT is compelled to stay close to the MPP during modest irradiance change. Therefore, loss of tracking direction is prevented. Another approach in [15] makes an additional power measurement without perturbation during the MPP searching. The difference between additional and perturbed samples includes both power changes that occurred by perturbation and the irradiation change. The power difference is determined assuming constant irradiation during a sampling interval. By calculating inaccuracies in this power difference, the algorithm may avoid confusion due to quickly changing irradiation. Another adaptive P&O algorithm with dynamic perturbation size is given in[16], combining traditional P&O and FSCC techniques. This approach, by contrast, utilizes current perturbation rather than voltage perturbation to improve tracking performance. Because the MPP's left-hand side is nearly constant. In addition, the proposed algorithm employs the FSCC approach to identify a new operating point nearer to MPP. This approach is only engaged when irradiance or current change significantly. In [17], the perturbation size of the P&O technique is revealed using a fuzzy logic controller.

1.1.2. Intelligent Methods

Conventional methods are typically simple and easy to implement. However, these techniques only perform well under uniform irradiance. Therefore, smart methods have been developed to track MPP in non-uniform conditions. Several types of intelligent algorithms are inspired by nature, including soft computing or using artificial intelligence.

Grey Wolf Optimization (GWO) is a heuristic algorithm centered on the grey wolf's leadership structure and hunting habits. The leadership is modeled using four types of the grey wolf which are alpha, beta, delta, omega. The optimal solution is represented by the alpha. Consequently, beta and delta are given the second and third optimal approaches. The remaining possible solutions are considered to be omega. Searching for prey, surrounding prey, and attacking the prey are the three main processes of GWO. These steps are used to develop GWO in order to achieve optimization [18]. Although the GWO algorithm reduces oscillation in steady and transient states and improves tracking performance, it has disadvantages such as greater cost and a longer calculation time due to the wide search area [19].

Fuzzy Logic Control (FLC) has emerged as the most important and effective application of fuzzy logic theory [20]. The fuzzy theory is a way of describing language rules in a way that can be rapidly examined. The fuzzy logic controller analyzes the load's power at any given moment and calculates the power change as a voltage function[21]. Fuzzification, fuzzy rule, and defuzzification are the three steps of the fuzzy logic-based MPPT. The inputs of PV parameters are turned into linguistic variables during the fuzzification step. Defuzzification is a fuzzification inverting procedure that uses mathematical connections to extract linguistics. There are two significant advantages over earlier approaches, no requirement for a mathematical system model or any system knowledge, and controller design is entirely under human control. However, the adjustment complexity of the membership function and control rules and choosing an operating range are downsides of the FLC [19].

Particle Swarm Optimization (PSO) is a population-based search technique inspired by the movement of bird flocks. The PSO method keeps track of a swarm of particles, each representing a possible solution. Particles have a basic behavior: imitating surrounding particles' accomplishments and their own [22]. The key concept is that each PV module is considered a molecule, and MPP is regarded as a target to pursue. Each PV module interacts with its master controller to maintain track of the required MPP, and each module is a slave to a single master module. Fast-tracking in changing situations and precise GMPP tracking are merits of the PSO algorithm. Nonetheless, the objective function is difficult to define because it depends on particle velocity [19].

Simulated Annealing (SA) is based on the metallurgical process of Annealing. A guided stochastic search is used in the search process. If a possible operating point has more power than the last best operating point, it may be chosen as the new best operating point. However, if a weaker operating point has a high enough acceptance probability, it may be accepted as the new best operating point. This allows the approach to thoroughly scan the solution space and avoid local maxima when the searching neighborhood is limited in size. The search is controlled by an artificial temperature parameter that is decreased corresponding to a cooling plan. According to the authors, the SA algorithm indicates that it has decent performance in tracing global maxima [23].

The Ant Colony Algorithms were created by studying the foraging actions of ants. They can discover the quickest route between a food source and their nest. An ant colony is predicated on the idea that it can determine the shortest route between two places by using basic communications systems. During their journeys, they leave a pheromone on the land. The pheromone attracts other ants to the intended location. The amount of pheromone available determines the route taken by an ant.

Moreover, this pheromone has a diminished effect with time, the quantity of food discovered and the number of ants traveling this path. The ACS method is based on this behavior, in which a group of ants collaborates to solve a problem by passing information with pheromones. When deciding on their next movement, ants may evaluate their own and other ants’ experiences taken together as a colony to find the best option [24]. The greater number of ants ensures faster convergence speed and more efficient optimization. Although many ants can track under any condition, it causes a long computation time. In addition, simultaneous optimization at the same is a challenging assignment for the controller, and complicated estimations are drawbacks of ACA [19].

Another nature-inspired algorithm is Artificial Bee Colony (ABC). This algorithm is based on the behavior of bee colonies. The artificial bees are divided into three groups which are employed bees, onlooker bees, and scouts. The colony’s purpose is to locate the biggest supply of nectar [25]. Employed foragers go out seeking food supply and report back to onlooker bees waiting in the hive through dancing communication. When a worker bee’s food source is abandoned, it becomes a scout and begins looking for food again [26]. The ultimate goal is to collect information on the most plentiful food supply. The algorithm performs better when the number of employed bees in the group is more numerous. In PV systems, this foraging process is well used to find the MPP. However, there are just a few control parameters in this method. Although this is an advantage, it may decrease tracking speed and stuck in LMPP [19].

Cuckoo Search (CS) algorithm is another method influenced by nature. This method was created by researching cuckoo bird reproduction patterns. Instead of building their nests, these parasitic animals lay their eggs within those of other birds. Cuckoo birds will search for new potential nests by flying randomly. They will choose the ideal nest to increase the probability that their eggs will hatch and give rise to a new cuckoo generation. In some circumstances, the cuckoo bird may attempt to increase the hatching probability by placing its eggs in a suitable location and rarely throwing the host bird's eggs from the nest. However, the host bird may discover the different eggs and quit its nest [27]. The cuckoo’s reproductive technique includes inquiring for a suitable host nest. Animals pick directions when seeking food that can be represented using mathematical functions. The Le’vy flight is one of the most popular models. It determines the cuckoo’s nest finding movements in CS. The Le’vy flight is a random process in which the levy distribution determines the step sizes [28]. According to [19], this approach has the advantages of a fast convergence rate as well as better efficiency.

An artificial neural network (ANN), a computational model, is based on biological neural network structure and functions. ANNs come in a variety of architectures. On the other hand, the feed-forward network is the most commonly used ANN. Information goes single direction through connected routes in a feed-forward network, from the input layer to the output layers. The significant benefit of an ANN is that it can learn from its experience. A neural network may be designed using the characteristics of the PV system for tracking the maximum power. At varying temperatures and irradiances, a correctly trained neural network can supply the maximum power [29]. Unfortunately, the necessity of system information for training and archiving massive amounts of data which increases the cost of the system, are drawbacks of this method [19].

A genetic algorithm (GA) is an optimization method inspired by the natural selection principle. GA performs a random search to solve an optimization problem. The initial condition does not affect the success of optimization. Selection, crossover, and mutation are the essential operators of genetic algorithms used to optimize the solutions [30].

In the sine-cosine algorithm, initially, partial shading is detected, and then an improved sine cosine algorithm is used to find the maximum power point of the photovoltaic array. In partial shading detection, the array voltage is scanned between the zero and open-circuit voltage. Then, partial shading conditions were determined by examining these voltage and corresponding power values. In the second part of this algorithm, the authors developed a random search algorithm based on the sine cosine algorithm (SCA). The authors reduced random factors from SCA. Therefore, the power fluctuation of the PV array is decreased while searching global maximum power point in PSC. The algorithm is studied through simulation and experimented with a 2-kW photovoltaic system. The paper concludes that the suggested method surpassed the GA and PSO-based partial shading detection solutions in the literature [31]. However, there are some considerable uncertainties about the proposed algorithm. The main weakness of this study is the method of PSC detection. Because the algorithm initially sweeps voltage through the operating voltage of the PV system to determine maximum power points. GMPP can already be determined with this step. The PSC detection algorithm makes the improved SCA unnecessary. In addition, there is no explanation for finding the number and values of the initial parameters of the algorithm in the paper.

In [32] the authors underline that there are multiple peak points under PSC, and conventional MPPT technique are unable to find a maximum power point. This problem is solved by the proposed two-stage MPPT approach. In the first step, a partial shading condition is determined. Three criteria are compared to the threshold values for determining PSC. Derivatives of PV array power, MPP voltage of array and MPP voltage of module are used to calculate these criteria. In the second stage, the authors prefer to P&O method for tracking MPP. In addition, ramp voltage is used on boost converter in PSC. Unlike the step command, settling time and transient are close to zero when ramp voltage is applied to the boost converter. Therefore, the power and voltage of the system may be measured continuously simultaneously in the ramp voltage phase. Thus, the proposed algorithm scans power points rapidly in order to find MPP in PSC. According to the authors, this algorithm has been verified by simulation and experimentation [32].

The algorithm given in [33] provides a method for tracking the global maximum power point based on shade detection and the trend of slopes from each part of the curve. The inclined and declined slopes on each part of the P-V characteristic curve form the basis of this algorithm's idea. First, the PV array curve is separated into parts based on the module's open-circuit voltage. Then, the system computes the reference point for the slope calculation. The slope computation selects a multiple of each open circuit voltage in the scaling ratio-deducted zone. Finally, GMPP is determined according to the calculated slopes.

1.1.3. Summary

A good MPPT algorithm must track MPP with a fast convergence speed under different weather conditions. Additionally, a good algorithm is expected to utilize low computational power and require as few sensors as feasible. Thus, hardware implementation of the good algorithm may be simple and affordable. Many researchers have attempted to develop algorithms that include the characteristics of a good algorithm. MPPT algorithms may be classified into three categories: conventional, intelligent, and hybrid. These types of methods have their benefits and drawbacks. Generally, conventional techniques are cost-effective and straightforward to implement in PV systems. Although the conventional technique may perform well under uniform irradiance, it struggles to detect GMMP in variable weather conditions. Also, the steady-state oscillation causes decreasing power extraction in conventional approaches such as P&O and IC methods. Many intelligent algorithms have been developed to overcome these drawbacks. Intelligent methods find GMPP by utilizing various complicated processes in all atmospheric conditions, especially partial shading conditions.

Moreover, PV systems can produce constant power at MPP by applying intelligent algorithms to prevent power fluctuation. However, intelligent techniques are more complex and challenging to implement. These methods are usually preferred by unique systems such as satellites and large power plants since intelligent approaches increase the cost of systems. Combining the advantages of the different types of algorithms to create a hybrid algorithm might result in a more successful solution.

2. PV MODELLING

2.1. PV CELL

A photovoltaic cell is a device that converts sunlight into electrical energy by using the photovoltaic effect. The characteristics of the photovoltaic cell vary depending on the amount of light energy exposed. Semiconductor silicon wafers are the basis of PV cells. The semiconductor is composed of p-type and n-type materials. The p-type and n-type semiconductor material forms a p-n junction by joining together. The exposed sunlight energy generates electrons traveling to p-type and holes traveling to n-type if the exposed energy is higher than the bandgap energy. The movement of the electrons and holes creates an electrical field. The working principle of the PV cell is demonstrated in Figure 2.1.

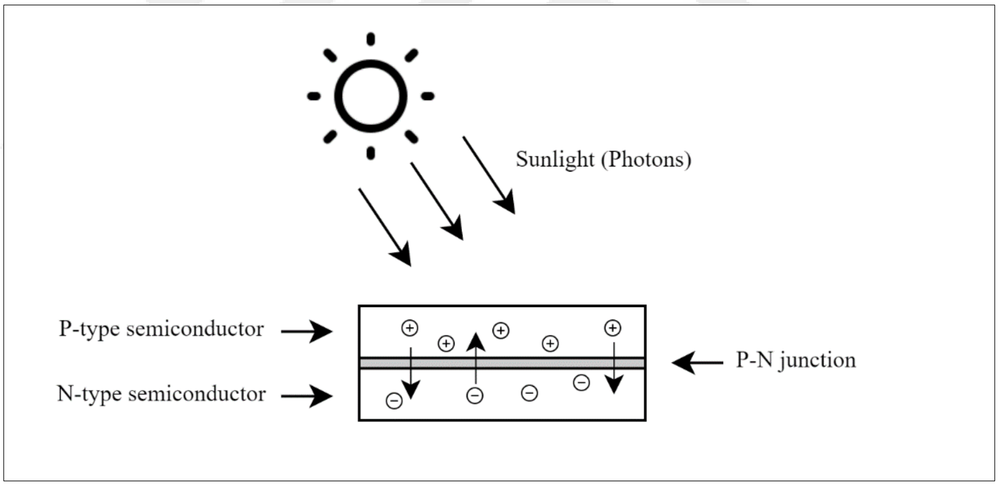

Figure 2.1. PV cell

An equivalent electrical circuit can be used to model the characteristic of the PV cell. In the literature, several models are utilized to represent the equivalent circuit of a PV cell. Figure 2.2. shows the equivalent circuit of an ideal PV cell model, which includes a current source and a diode. The diode reflects the p-n junction behavior of the PV cell. Also, the light-generated current is represented by a current source.

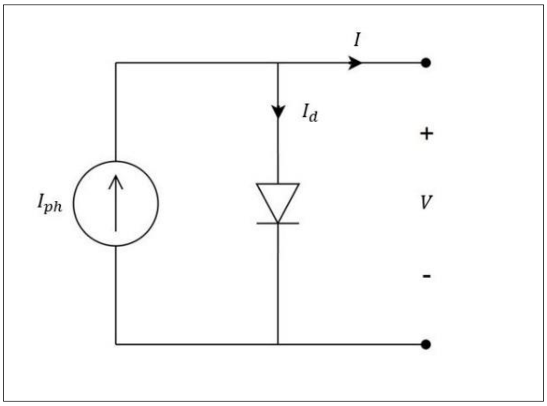

Figure 2.2. Equivalent circuit of an ideal solar cell model

In several studies, for instance [34], [35] and [36], the model is shown in Figure 2.2. has been named as the ideal PV cell model, but it should be noted that a non-ideal diode is used in the ideal solar model in these studies. Assuming the diode used to represent the solar cell is ideal, it affects the slope in the region near the MPP in the current-voltage characteristics of the ideal solar model, as indicated in Figure 2.3.

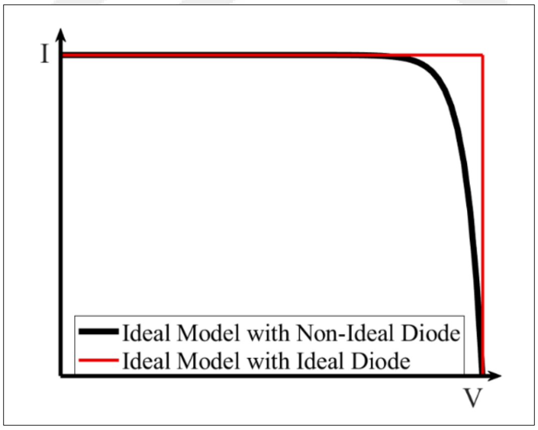

Figure 2.3. Effect of the ideal diode on Current-Voltage characteristic of ideal solar cell

Kirchhoff's current law may be used to write the current-voltage characteristic equation of an ideal model, which is given by Equations (2.1) and (2.2).

$$I = I_{ph} - I_d \tag{2.1}$$

$$I_d = I_0 \left[\exp\left(\frac{V}{V_t}\right) - 1 \right] \tag{2.2}$$

where I_{ph} is light-generated current, I_0 is reverse saturation current. Also, V_t is the junction voltage in Equation (2.3).

$$V_t = \frac{akT}{q} \tag{2.3}$$

where, k is Boltzmann constant, T is junction temperature, a is diode ideality factor, and q is the electron charge.

The current-voltage characteristics of a real PV cell cannot be adequately represented by the ideal solar cell model in Figure 2.2. Unlike the single diode model, the ideal solar cell model does not consider the losses and leakage current. By adding R_s and R_p resistors to the ideal solar cell model, a more accurate PV model known as the single diode model is developed, as shown in Figure 2.4. The difference in current-voltage characteristics between the ideal diode and the single diode model is indicated in Figure 2.3(b). Losses resulting from current flow and leakage current are characterized by R_s and R_p. Therefore, the single diode model is most often utilized because it balances accuracy and simplicity well [37].

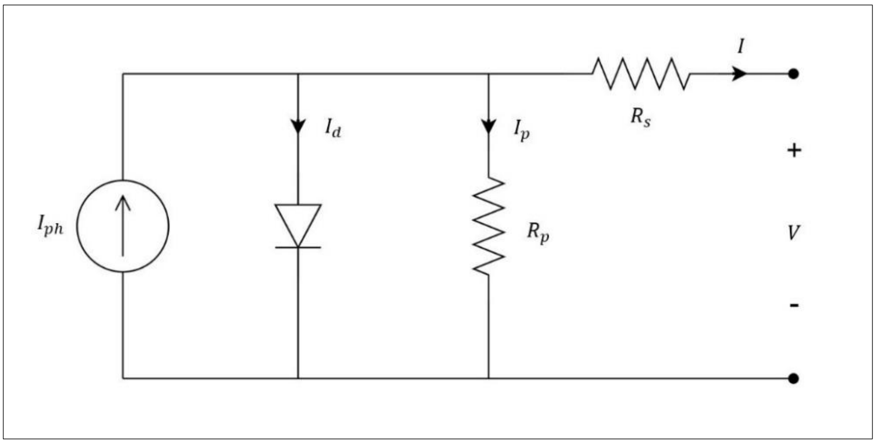

Figure 2.4. Equivalent circuit of single diode model

Equations (2.4) and (2.5) can be acquired using Kirchoff's current law and nodal analysis, respectively, from the equivalent circuit of the single diode model.

$$I = I_{ph} - I_d - I_p \tag{2.4}$$

$$I_p = \frac{V + IR_s}{R_p} \tag{2.5}$$

The Diode current of the single diode model (Equation 2.6) can be derived from Equation (2.2).

$$I_d = I_0 \left[\exp\left(\frac{V + IR_s}{V_t}\right) - 1\right] \tag{2.6}$$

By inserting Equations (2.5) and (2.6) into (2.4), the current-voltage characteristic equation given in Equation (2.7) is obtained.

$$I = I_{ph} - I_0 \left[\exp\left(\frac{V + IR_s}{V_t}\right) - 1\right] - \frac{V + IR_s}{R_p} \tag{2.7}$$

The slope of the current-voltage curves is mostly affected by R_s. Figure 2.5(a) illustrates the effect of changing the series resistance value on the I-V characteristics of the PV model. The approximation of R_s value is given by Equation (2.8) [38]:

$$R_s \approx -\frac{dV}{dI}\bigg|_{V = V_{OC}} \tag{2.8}$$

R_p has an effect on the curve slope at the current levels near the short circuit area. The impact of parallel resistance of the single diode model on I-V characteristics is shown in Figure 2.5(b). The approximation of R_p value is given by Equation (2.9) [38]:

$$R_p \approx -\frac{dV}{dI}\bigg|_{I = I_{SC}} \tag{2.9}$$

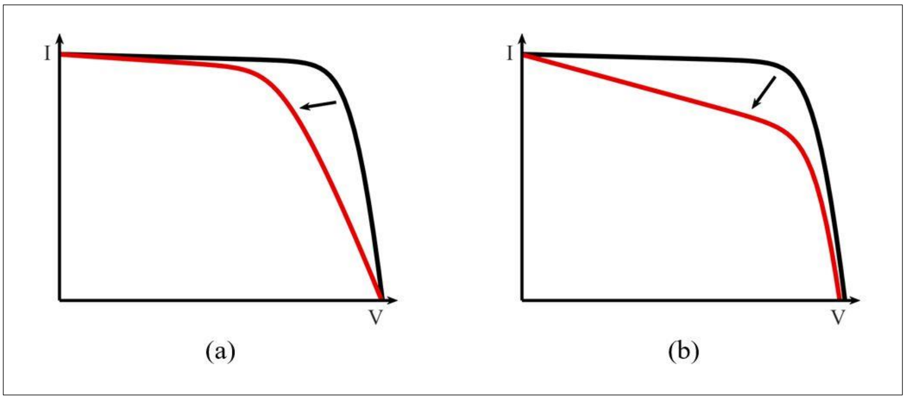

Figure 2.5. Voltage–Current characteristics of single diode model according to (a) Increasing the serial resistance (b) Decreasing the parallel resistance

Although the single diode model is the most common, the double diode model is more accurate. However, the impact of carrier recombination is represented by an additional diode which increases the number of unknown parameters, as shown in Figure 2.6. However, the double diode model is not widely used because of the complexity induced by increased unknown parameters.

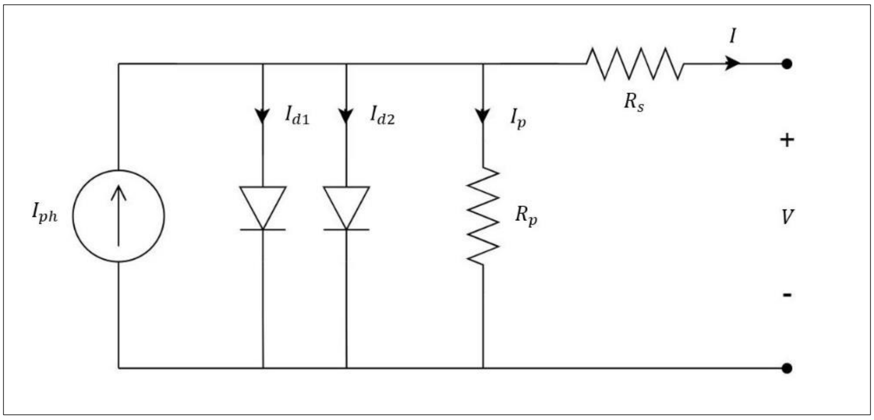

Figure 2.6. Equivalent circuit of double diode model

Similar to Equation (2.7), Equation (2.10) illustrates the current-voltage characteristics equation of a double diode model.

$$I = I_{ph} - I_{01}\left[\exp\left(\frac{V + IR_s}{V_t}\right) - 1\right] - I_{02}\left[\exp\left(\frac{V + IR_s}{V_t}\right) - 1\right] - \frac{V + IR_s}{R_p} \quad (2.10)$$

where I_{01} and I_{02} are reverse saturation currents of the two diodes.

Another important term related to PV models is the Fill Factor (FF). The FF is a measurement of a PV model's efficiency. Higher FF indicates the quality of the PV panel. The FF is described in Equation (2.11).

$$FF = \frac{V_{MPP}\, I_{MPP}}{V_{OC}\, I_{SC}} \tag{2.11}$$

Lower FF may be caused by decreased parallel resistance and increased series resistance, as seen in Figure 2.5.

Assuming the diode in the single diode model is ideal, the model may be examined in two different cases: diode voltage is less than the forward voltage of the diode (V_D) and diode voltage is equal to forward voltage.

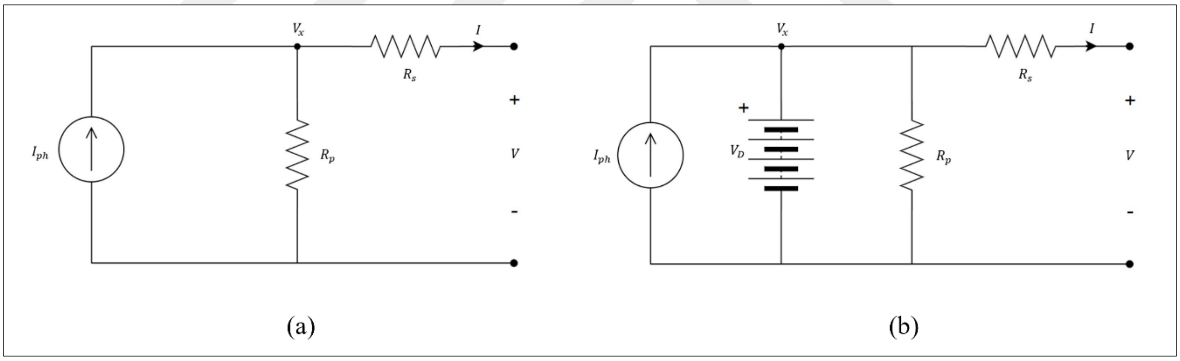

Figure 2.7. Equivalent circuit of single ideal diode model (a) Diode voltage below the forward voltage (b) Diode voltage above the forward voltage

In case the diode voltage drops below V_D, there is no current flow through the ideal diode, which is modeled as an open circuit. Therefore, the equivalent circuit of the single diode model becomes the circuit in Figure 2.7(a). Equation (2.12) can be written when the circuit is solved from the point V_x .

$$R_s I + V = R_p\left(I_{ph} - I\right) \tag{2.12}$$

When the diode voltage equal to V_D, the diode can be represented by a voltage source. Hence, the equivalent circuit in Figure 2.7(b) may be used instead of the single diode model. Equation (2.13) can be written when circuit analysis is applied to the circuit in Figure 2.7(b).

$$I = \frac{V_D - V}{R_s} \tag{2.13}$$

Equation (2.14) is derived from Equations (2.12) and (2.13):

$$I = \begin{cases} \dfrac{R_p}{R_s + R_p} I_{ph} - \dfrac{1}{R_s + R_p} V & , \quad V_x < V_D \\ \dfrac{1}{R_s} V_D - \dfrac{1}{R_s} V & , \quad V_x = V_D \end{cases} \tag{2.14}$$

The current-voltage characteristics of a single diode model with an ideal diode can be drawn using Equation (2.14), as shown in Figure 2.8.

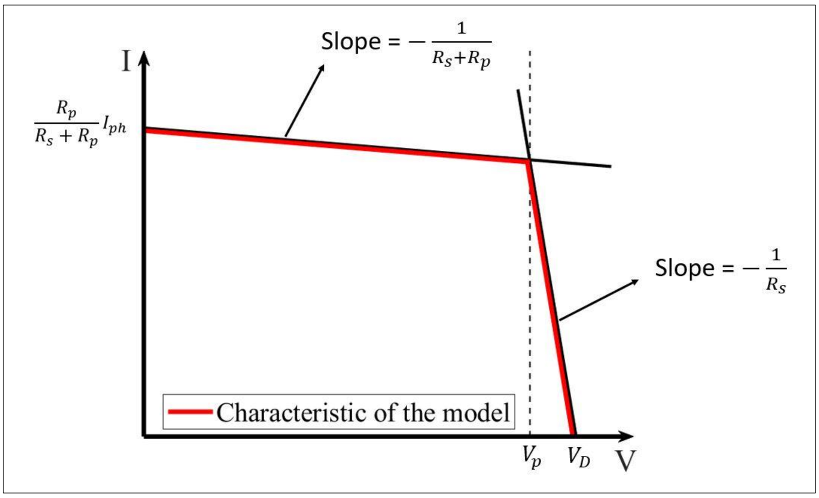

Figure 2.8. Characteristic of the single ideal diode model

The intersection point of two slopes can be found by equating Equation (2.14) as follows:

$$\frac{1}{R_s + R_p}\left(R_p I_{ph} - V_p\right) = \frac{1}{R_s} V_D - \frac{1}{R_s} V \tag{2.15}$$

When the above equation is arranged, V_p can be found in Equation (2.16).

$$V_p = \left(1 + \frac{R_s}{R_p}\right) V_D - R_s I_{ph} \tag{2.16}$$

The current-voltage characteristic in Figure 2.8. can be converted to power-voltage characteristic by calculating the power values. Equation (2.17) can be written for values V.

$$P = IV = \begin{cases} \dfrac{R_s}{R_s + R_p} I_{ph} V - \dfrac{1}{R_s + R_p} V^2 \quad , & V < V_p \\ \dfrac{V_D V}{R_s} - \dfrac{V^2}{R_s} \quad , & V_p < V < V_D \end{cases} \tag{2.17}$$

The power-voltage characteristic in Figure 2.3. is acquired from Equations (2.17).

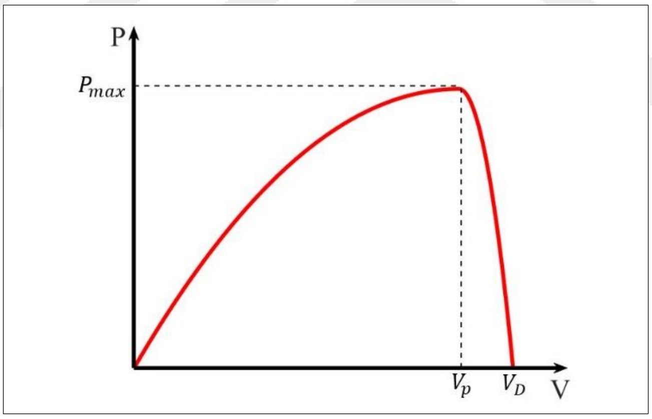

Figure 2.9. Power-Voltage characteristic of the single diode model

The maximum power is transferred from the cell when the terminal voltage is equal to V_p, as shown in Figure 2.9. Consequently, the corresponding voltage value of the maximum power point can be derived from the characteristic equation of the PV cell.

2.2. PV MODULE

PV panels are formed by many cells connected in series. Conventional full-size PV module usually consists of 60 or 72 cells with three bypass diodes. Thus, modules may produce a higher power output. As an example, the PV module consists of 60 cells and is divided into three submodules, as shown in Figure 2.10(a).

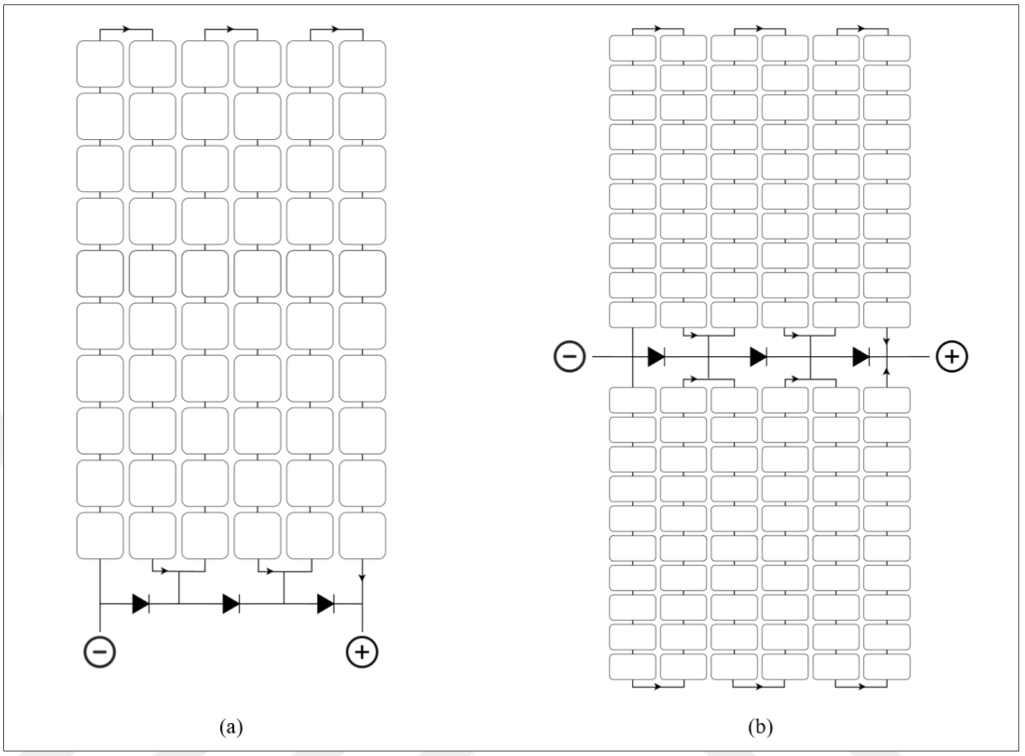

Figure 2.10. PV modules with bypass diode (a) Conventional module (b) Half-cut module

Bypass diodes are connected parallel with submodules to prevent PV cells from being damaged in partial shading. Shaded cells generate more current than unshaded cells in partial shading conditions. Hence, the current produced by the unshaded cells tries to pass through the shaded cells. As a result, the shaded cell consumes power instead of producing power. Consequently, the cell mat heats up and gets damaged. However, the current generated by the unshaded panel is transferred without damaging the cells due to bypass diodes.

Half-cut panels typically include 120 to 144 cells formed by cutting cells in half, as shown in Figure 2.10(b). The solar cells are cut in half, and the currents are correspondingly halved, reducing the resistive loss. Therefore, PV cells may produce more power which increases panel efficiency. Furthermore, the half-cut modules can produce more power than conventional panels in partial shading. When a cell is shaded in a conventional module, the entire row of cells connected in series cannot generate power. Only one cell shadowing causes a third of the panel to be lost since there are three rows. However, if a row is shaded in a half-cut panel, the opposite row can still generate power, resulting in a one-sixty power loss. Half-cut modules work as two half-modules. When the lower half of the panel is shaded, the panel continues to generate half of the total current due to the diode placement. In addition, hot spots on half-cut panels are less likely to cause harm [39].

There are various structures in PV modeling. The basic structure of photovoltaics is PV cells. A group of PV cells is connected in series to create a PV module or panel. A string consists of many series connected modules to produce a higher voltage. The strings are wired in parallel or series to form the array depending on the current or voltage requirements.

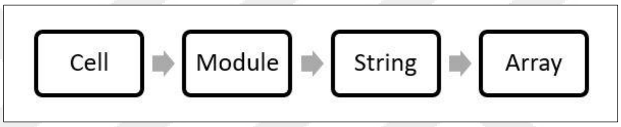

Figure 2.11. PV structures

The PV structures are demonstrated in Figure 2.11. according to their power capacities from low to high.

2.3. SIMULINK PV MODEL

In this study, the PV array block (see Figure 2.12.) from the Simulink library was used to analyze the MPPT algorithm. PV model in Simulink utilizes System Advisor Model's (SAM) California Energy Commission (CEC) module model. SAM is open-source modeling software for performance or financial analyses that helps individuals in the renewable energy sector make good decisions. to CEC module model is an implementation of De Soto's [40] single diode model.

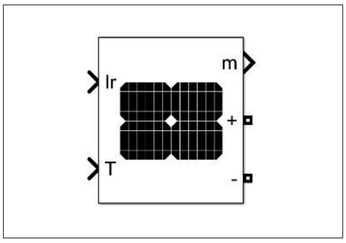

Figure 2.12. PV array block in MATLAB Simulink

The PV array block is based on the single diode model (see Figure 2.13.) or the five-parameter model, whose characteristics equation is given in Equation (2.7). Five parameters are I_L or I_{ph}, I_0, R_S, R_P and α in Equation (2.7). However, this equation is valid under ideal conditions. CEC module models consider temperature and irradiance change effects with auxiliary equations. Auxiliary equations include parameters of the single diode model.

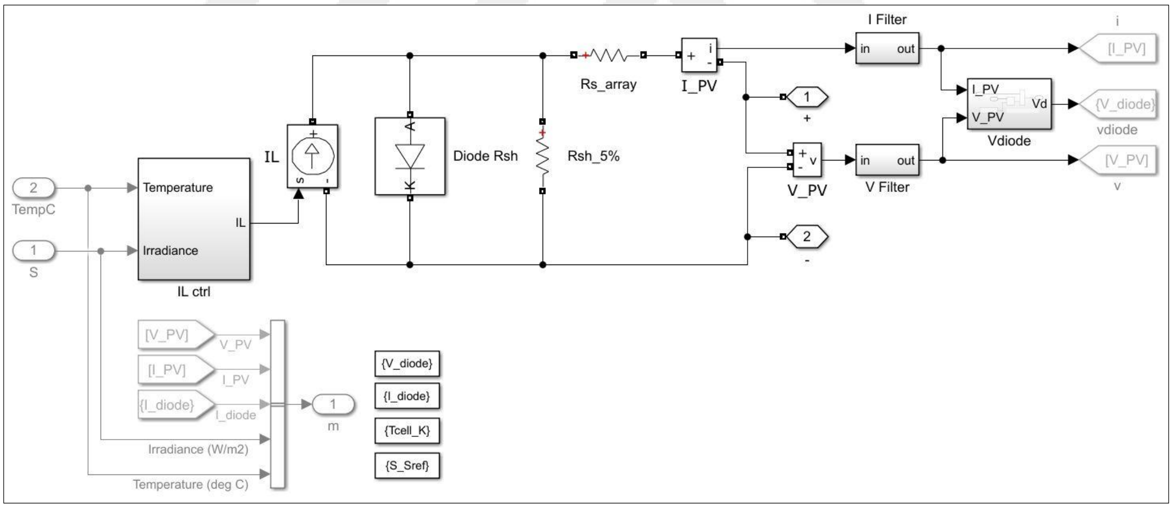

Figure 2.13. Model of PV array block in MATLAB Simulink

The light-generated current is affected by temperature and irradiance. The light-generated current can be subtracted from any temperature and irradiance value with Equation (2.19). Also, the $adjust$ parameter, calculated from the CEC module library or SAM's coefficient generator, is used to adjust the temperature coefficient of short circuit current (μ_{isc}). In Equation (2.20), adjusting the temperature coefficient of the short circuit is given.

$$I_L = \frac{S}{S_{ref}}\left(I_{L,ref} + \mu_{isc}\left(T_c - T_{ref}\right)\right) \tag{2.19}$$

$$\mu_{isc} = \alpha_{sc,ref}\left(1 - \frac{adjust}{100}\right) \tag{2.20}$$

where I_L is photocurrent, S irradiance, T_c is cell temperature, T_{ref} and S_{ref} are equal to, respectively, 25℃ and 1000 W/m^2. Figure 2.11 shows that the light-generated current was modeled with a controlled current source controlled by a function block. The function block contains mathematical blocks corresponding to Equation (2.20), as shown in Figure 2.14.

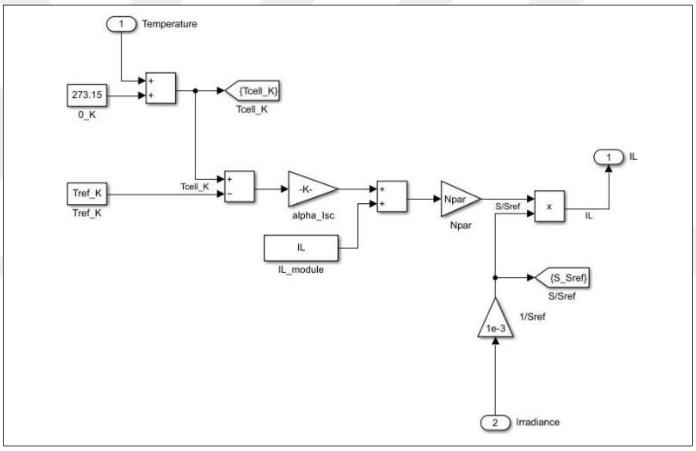

Figure 2.14. Light-generated current block in MATLAB Simulink

The parts of the diode model are shown in Figure 2.15. and 2.16. I_0, R_P and V_t are modeled in the figure below.

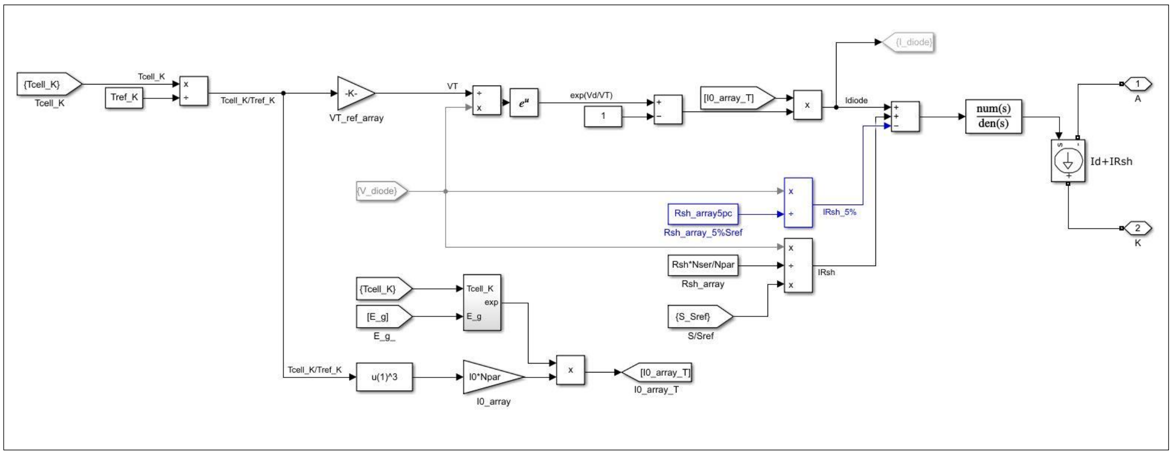

Figure 2.15. Part of a diode block in MATLAB Simulink

The equation for the reverse saturation current is given by:

$$I_0 = I_{0,ref}\left(\frac{T_c}{298.15}\right)^3 \exp\left[\frac{1}{k}\left(\frac{1.12}{T_{c,ref}} - \frac{E_{bg}}{T_c}\right)\right] \quad (2.21)$$

where k is Boltzmann constant $k = 8.618\, x\, 10^{-5}\, eV/K$, $E_{g,ref}$ is reference bandgap energy $E_{g,ref} = 1.12\ eV$, reference cell temperature is $T_{c,ref} = 298.15\ K$.

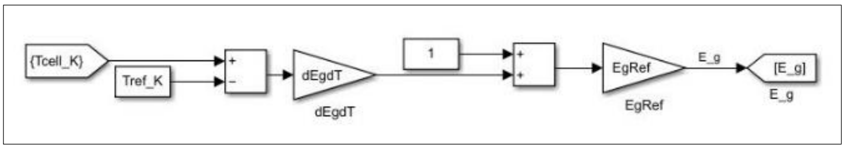

Figure 2.16. Bandgap energy equation block in MATLAB Simulink

The modeling of bandgap energy changes according to temperature is demonstrated in Figure 2.16. The bandgap energy is calculated to Equation (2.22).

$$E_{bg} = 1.12[1 - 0.0002677(T_c - T_{c,ref})] \quad (2.22)$$

The parallel resistance of the single diode model is affected by changes in irradiance given in Equation (2.23). Also, the series resistance R_S is assumed to be constant.

$$R_P = R_{P,ref} \frac{1000}{G} \tag{2.23}$$

The temperature change affects the diode ideality factor of a single diode model as in Equation (2.24).

$$\alpha = \alpha_{ref} \frac{T_c}{T_{c,ref}} \tag{2.24}$$

Consequently, the CEC module model provides more accurate results in temperature and irradiance changes by using auxiliary equations that include five parameters of a single diode model with the equation of characteristic of a single diode model.

The PV model of Simulink takes temperature and irradiance values from outside the PV panel (see Figure 2.12). This temperature value is used directly as the cell temperature value, as indicated in the PV cell blocks. However, in practice, monitoring ambient temperature is simpler and more affordable. As a result, the cell temperature may be calculated from the ambient temperature. Therefore, the relationship between solar cell temperature and ambient temperature is calculated using Equation (2.25) [41].

$$T_{cell} = T_{air} + \frac{NOCT - 20}{80} G \tag{2.25}$$

where T_{cell} is the cell temperature, T_{air} is the ambient temperature, $NOCT$ is the nominal operation temperature, and G is irradiance. Equation (2.25) is integrated into the PV model, as shown in Figure 2.17.

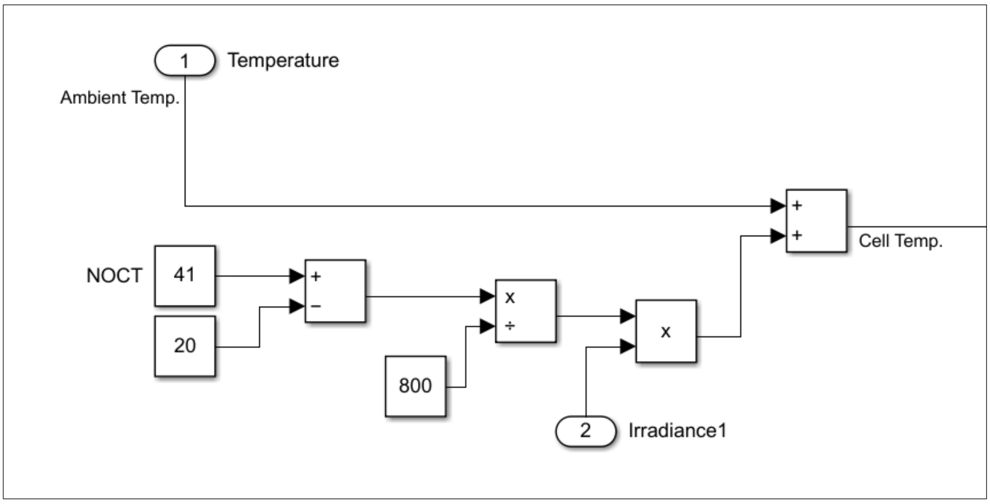

Figure 2.17. Blocks for calculating cell temperature in Simulink

2.3. PV CHARACTERISTICS

The form of the PV system characteristics is affected by irradiance and temperature. PV array may not be exposed to uniform irradiance due to environmental factors. Non-uniform irradiance on the module may be caused by trees and building shadows, clouds, and dirt on the panel. The cells in the panel cannot produce the same amount of current in partial shading conditions. The cells are forced to generate as much current as the poor cell. Therefore, the PV module produces less power, and poor cells may be damaged due to overheating. Bypass diodes are utilized to obtain more power and prevent panel damage. Under PSCs, multiple local maxima may occur in the PV output characteristic due to the current flowing through the bypass current. The PV characteristic is affected by shadow intensity, location of bypass diode, and module configuration in case of partial shading.

The bypass diode can be used inside and outside the PV module. Although using a diode in each cell in the PV module is more effective, bypass diodes are connected to a certain number of cells connected in series because of the cost (see Figure 2.10.). The half-cut module layouts with three diodes in various shading patterns are shown in Figure 2.18.

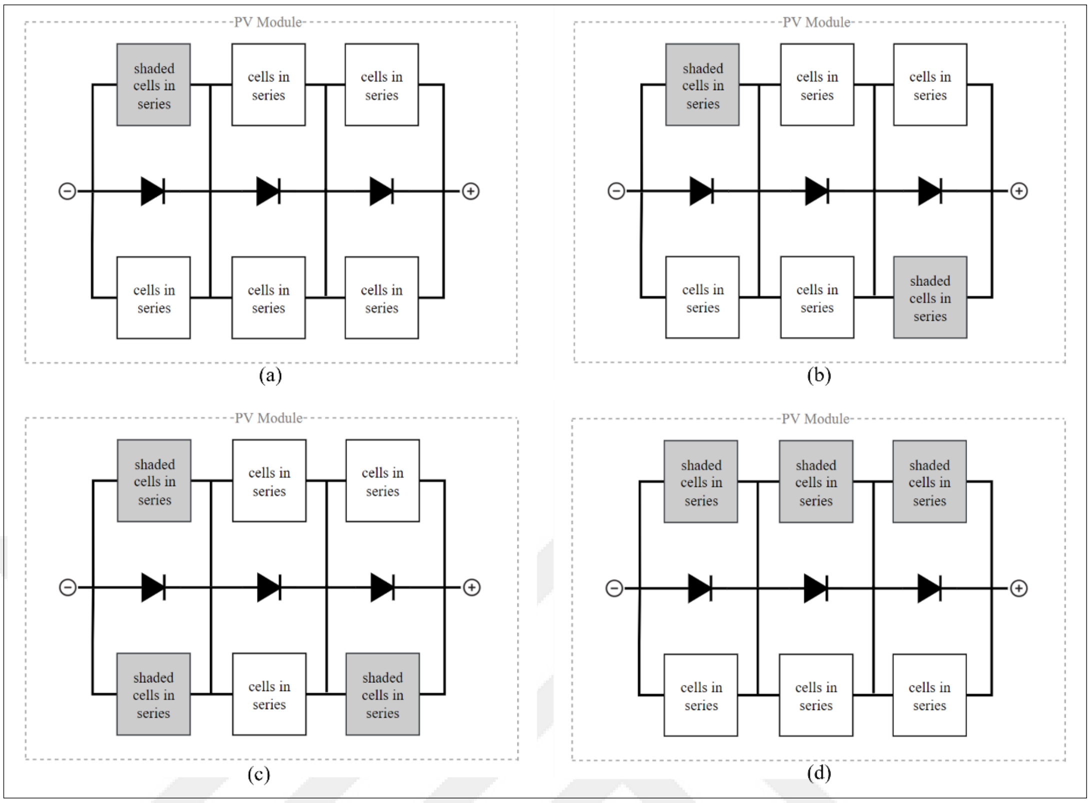

Figure 2.18. Half-cut PV module layout under different shading patterns (a) one shaded group cells in series with 500 W/m^2 (b) two shaded groups in series with 200-400 W/m^2 (c) three shaded groups in series with 400-100-200 W/m^2 (d) three shaded groups in series completely shaded

The half-cut PV module from a well-known manufacturer, whose parameters are listed in Table 2.1, was utilized in MATLAB Simulink software to analyze the characteristics of the PV module in PSC.

Table 2.1. Specification of PV module used in this study

Parameter	Values
Nominal maximum power P_{max} (W)	580
Open circuit voltage V_{OC} (V)	40.5
Short-circuit current I_{SC} (A)	18.27
Voltage at maximum power point V_{MP} (V)	34.1
Current at maximum power point I_{MP} (A)	17.02
Temperature coefficient of V_{OC} $(\%/°C)$	-0.34
Temperature coefficient of I_{SC} $(\%/°C)$	0.05

Figure 2.18(a) indicates that shadowing in the PV module affects a part of the series-connected cells. Although unshaded cells receive $1000W/m^2$ irradiance, shaded cells receive $500W/m^2$ irradiance, causing partial shading conditions.

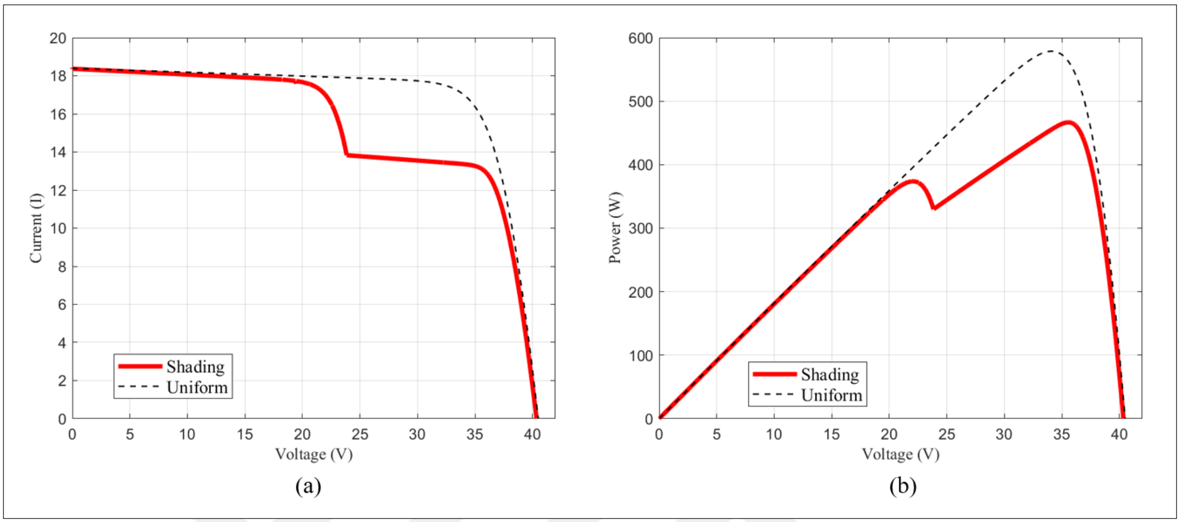

Figure 2.19. Characteristics of the module in partial shading condition (a) current-voltage characteristic (b) voltage-power characteristic

The effect of the bypass diode on the I-V characteristic of the PV module can be seen in Figure 2.19(a). The P-V curve has two peaks that can be seen in Figure 2.19(b) because of the bypass diode, but one of them is the global maximum power point. The location of peak points may change according to the irradiance level and pattern.

In Figure 2.18(b), two shaded groups of series cells received 200 and 400 W/m^2 irradiance, while three shaded series cells groups in Figure 2.18(c) are lit by 400-100 and 200 W/m^2 of solar insolation. Other cells are also illuminated with $1000W/m^2$ irradiance. The effects of these shading patterns and solar insolation levels on I-V and P-V characteristics can be seen in Figure 2.20.

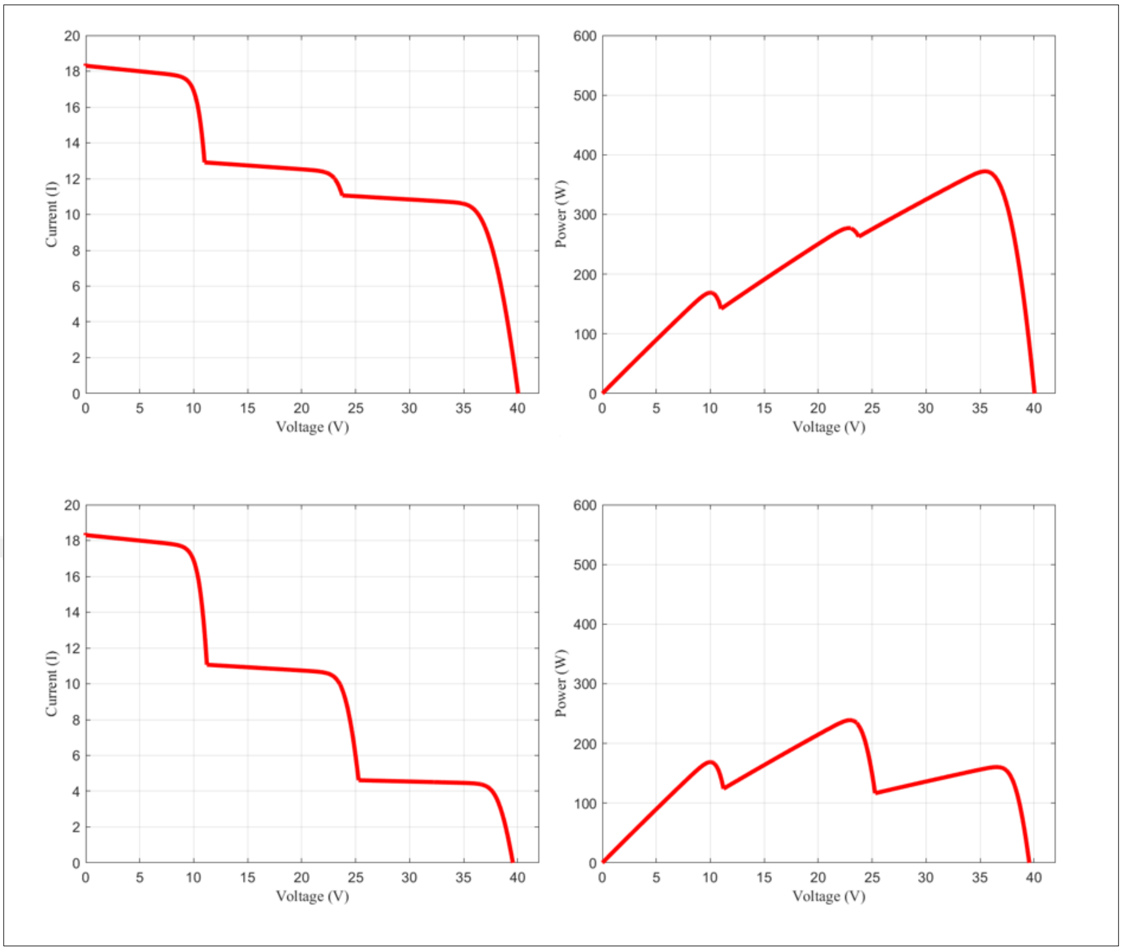

Figure 2.20. Characteristics of the half-cut module in various partial shading conditions

The half-cut panel's upper half is fully darkened, while the other half is illuminated with 1000w/m2 irradiance, shown in Figure 2.18(d). However, due to its unique wiring design, the half-cut panel may produce half the current it can generate in total, as shown in Figure 2.21.

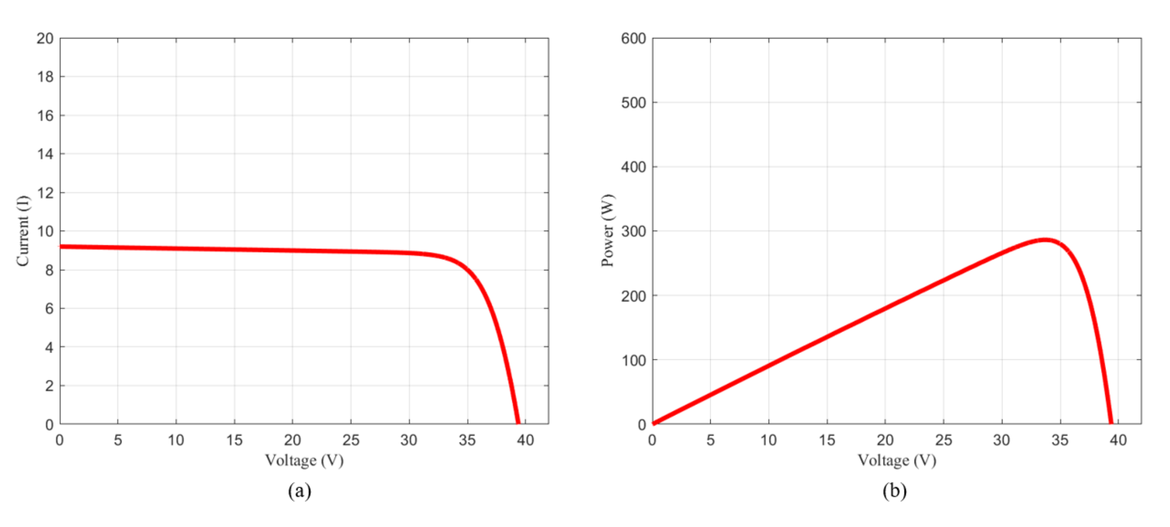

Figure 2.21. Characteristics of the half-cut panel when half of the panel is shaded

3. MAXIMUM POWER POINT TRACKING ALGORITHMS

The I-V and P-V characteristics of the PV panels are unique, and the form of panel characteristics changes depending on irradiance and temperature. Therefore, the positions of the maximum power points continuously vary in different environmental conditions. To extract maximum power, the PV panel must operate at its maximum power point. Therefore, it is necessary to track the maximum power point in order to achieve optimum efficiency. There are numerous MPPT methods in the literature [3,4]. However, these algorithms range from simple to complex and can only work in uniform irradiation to partially shaded conditions. The MPPT methods and their classification are indicated in Figure 3.1.

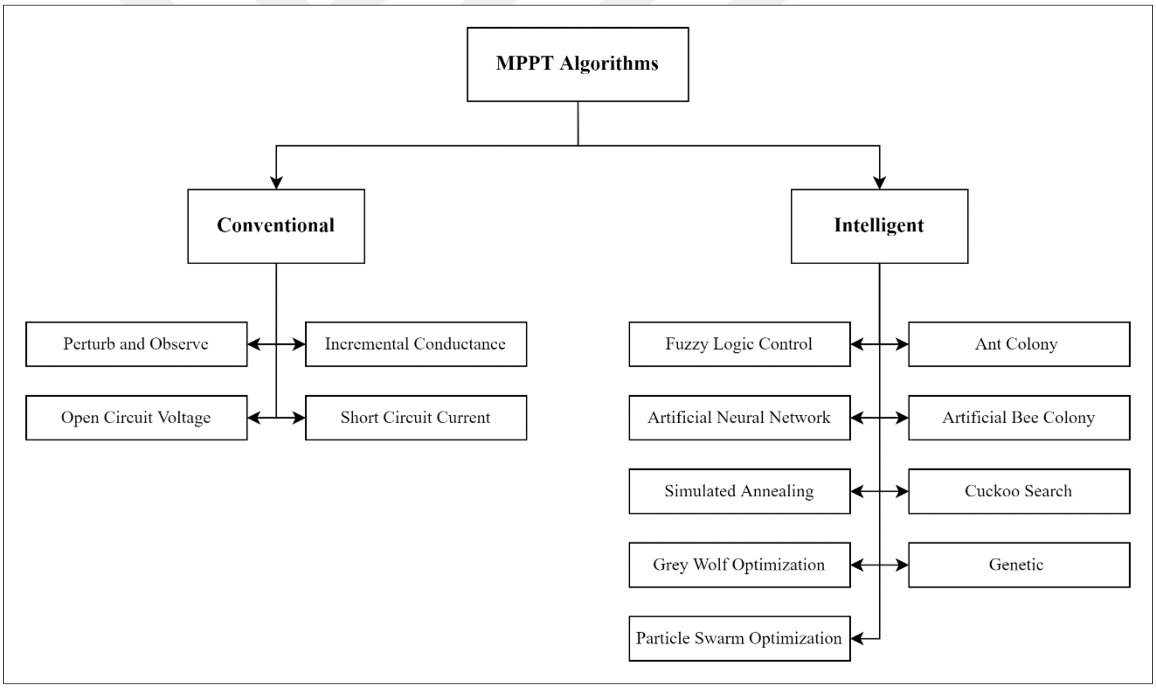

Figure 3.1. Classification of MPPT Methods

The algorithm presented in this thesis is based on the perturb and observe method and compared with the simulated annealing algorithm. Hence, these methods are clearly explained in the next section.

3.1. PERTURB AND OBSERVE METHOD

The P&O method is one of the most widespread approaches, which stands out from conventional models with its quick convergence to MPP. In the P&O technique, the operating voltage of the PV panel is perturbed in one direction, and it is checked whether the power increases or not. If there is an increase in power, perturb continues in the same direction, otherwise, perturb is performed in the other direction. Figure 3.2. shows the flowchart of the P&O technique.

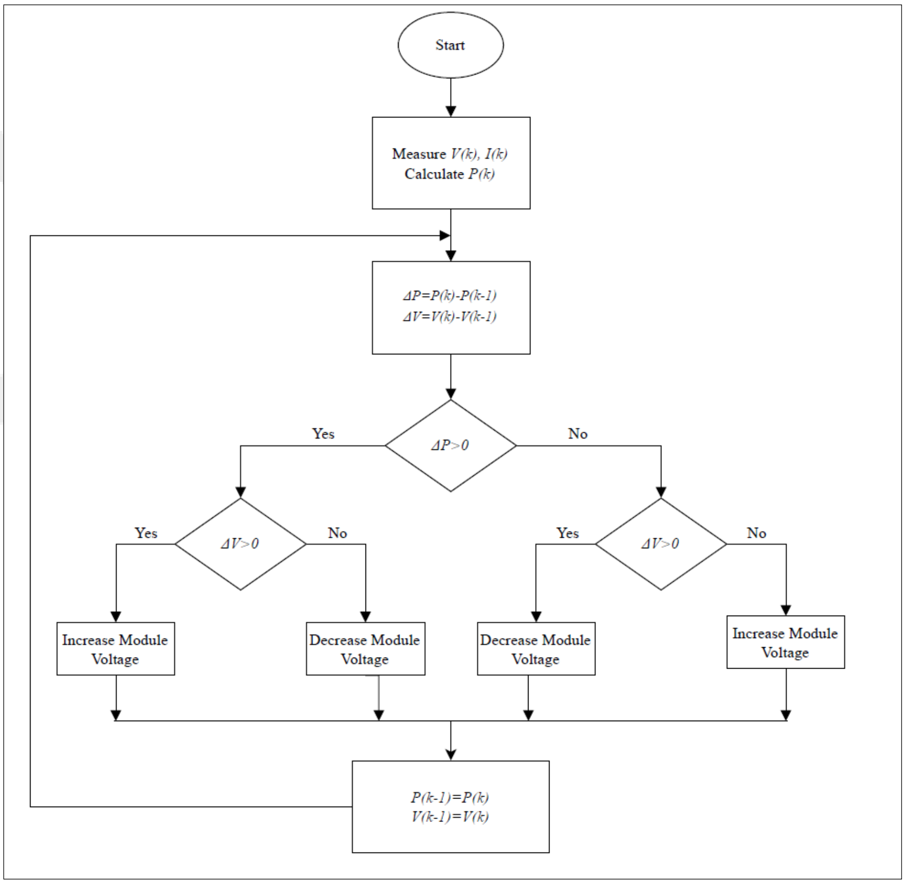

Figure 3.2. Flowchart of the perturb and observe method

The perturbation size is the main factor that affects the performance of the P&O algorithm. Large perturbation size causes power loss by creating high oscillations. On the contrary, a small perturbation size reduces tracking speed. Thus, this approach requires a trade-off between power loss and tracking speed. More crucially, the P&O method fails to detect the global peak under partially shaded conditions because the algorithm is stuck on LMPPs.

3.2. SIMULATED ANNEALING METHOD

Simulated Annealing is one of the metaheuristic methods. SA takes its cue from the metallurgical annealing process, in which the metal is easily deformed at high temperatures but becomes more challenging as the temperature drops. In order to adopt SA, choosing the right temperature is crucial [42]. The flowchart of the simulated annealing algorithm is demonstrated in Figure 3.3.

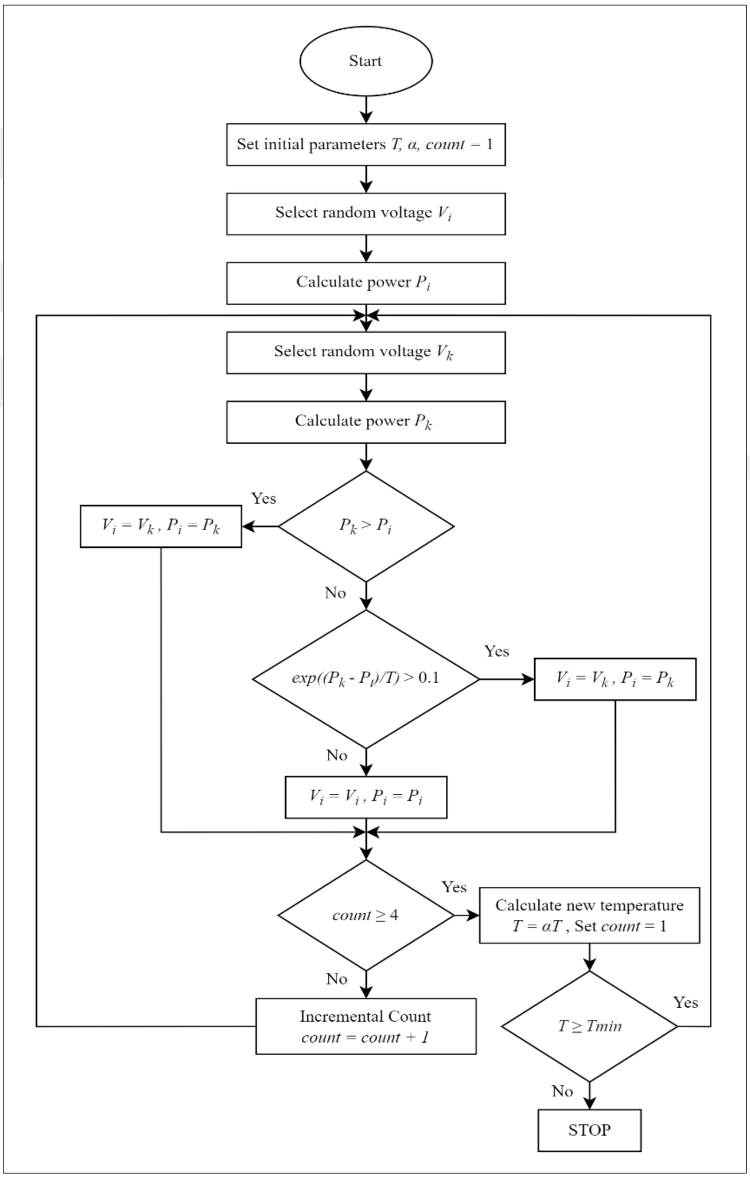

Figure 3.3. Flowchart of the simulated annealing method

A cooling rate, final temperature, and initial temperature are necessary for the SA algorithm. The technique adjusts voltage multiple times at each temperature and measures the corresponding power. Then, a comparison is made between the measured power and the current reference power. It will be selected as the new operating point if the new position has more energy. Moreover, depending on the acceptance probability, the new operating point may still be selected even though it has lower power than the reference operating point [43].

The Simulated Annealing algorithm successfully locates the GMPP in different shading conditions. However, power loss occurs throughout the GMPP search due to the long convergence time. Moreover, changing irradiance during a GMPP search may cause the SA algorithm to find an incorrect location.

4. METHODOLOGY

4.1. PARTIAL SHADING EFFECTS ON HALF-CUT PANEL WITH THREE BYPASS DIODES

As discussed in previous sections, several peak points may occur on the panel characteristics in partial shading conditions. These peaks may emerge because the unshaded part of the panel creates more current than the shaded part, which is transmitted to the line through the bypass diodes. Thus, the link between the number of peaks and bypass diodes is explained. The number of peaks in the panel's characteristic can be as much as the number of diodes. Depending on the shading pattern, there can be two or three maxima in the characteristics of the half-cut panel with three bypass diodes. The P-V characteristic graph of the half-cut panel with two maxima at varied insolation levels is shown in Figure 4.1.

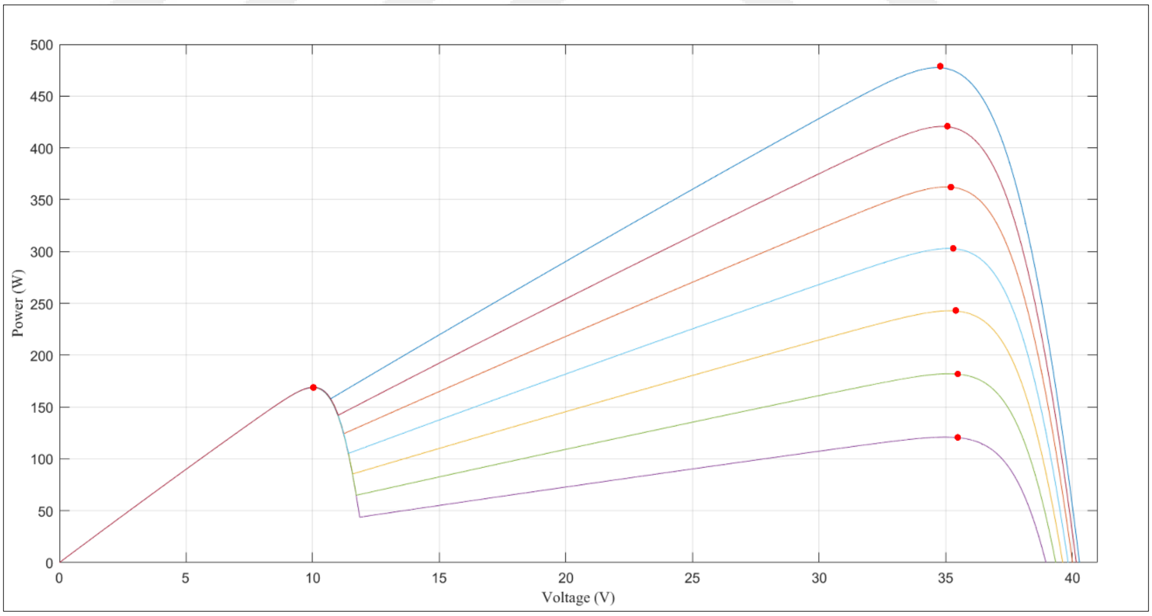

Figure 4.1. P-V characteristic graph of the half-cut panel with two maxima in variable insulation

When the red dots representing the peaks in Figure 4.1 are analyzed, it is seen that the two peaks formed in variable irradiance are around 10 and 35 volts. Figure 4.2 illustrates the P-V characteristic graph of a panel shaded in another shape with various irradiance.

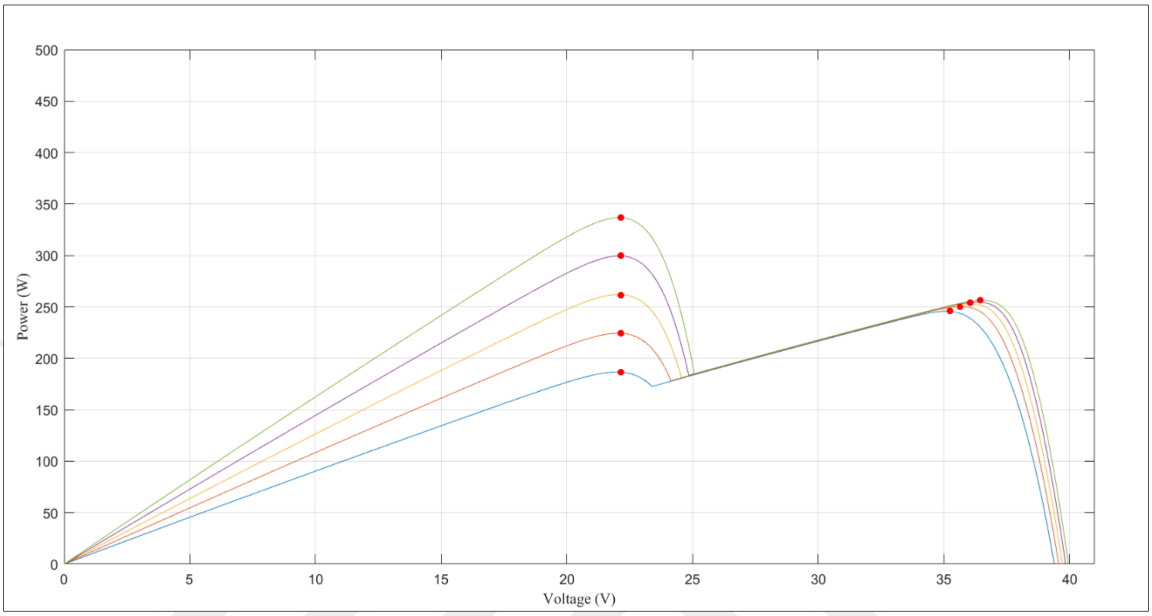

Figure 4.2. P-V characteristic graph of the half-cut panel with two maxima in another shading shape with varied insulation

It is seen in Figure 4.2 that the maxima of the P-V graph occur around 23 and 36 volts.

A P-V characteristic of the panel with three peaks can be formed in varied shading patterns and irradiation, as shown in Figure 4.3.

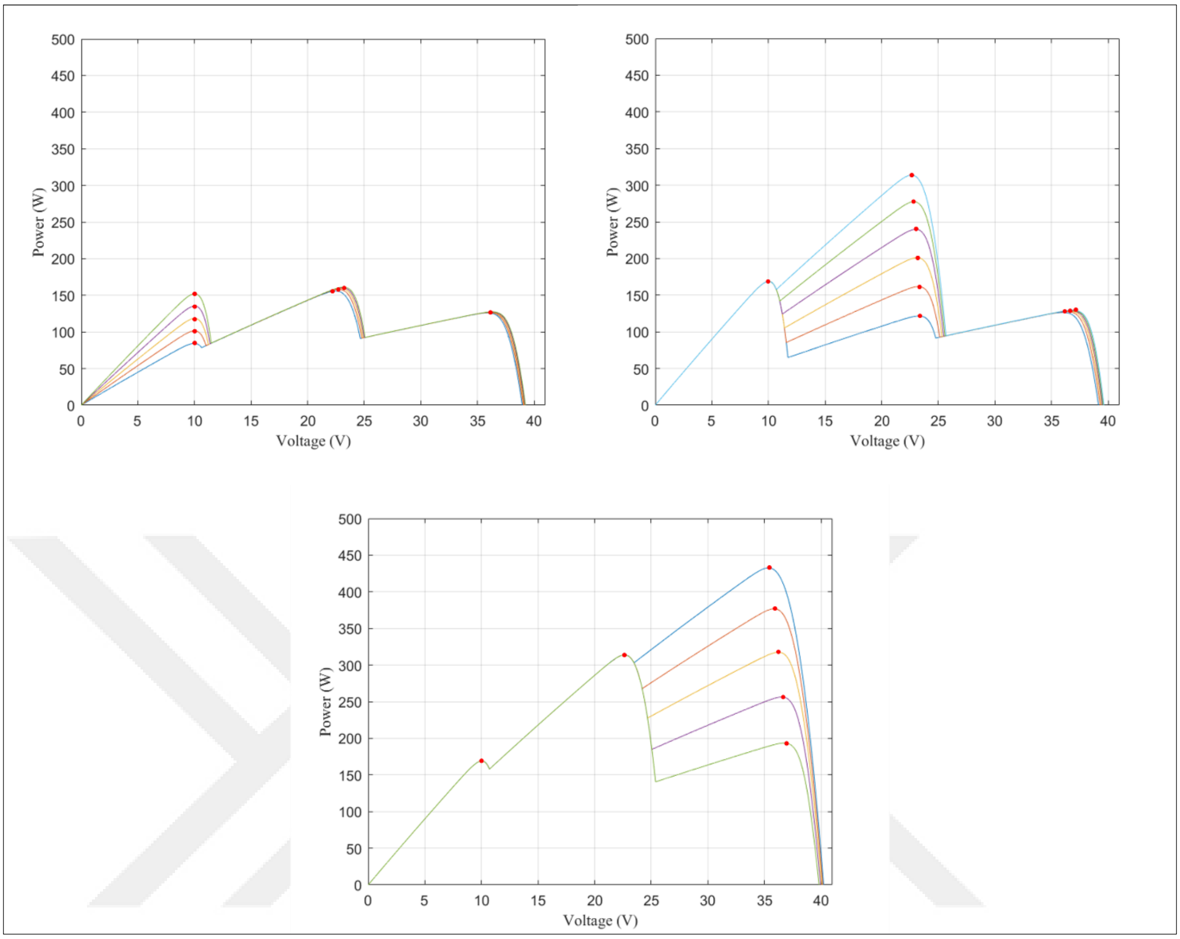

Figure 4.3. P-V characteristic graphs of the half-cut panel with three maxima in various shading patterns and irradiance

Figure 4.3 shows that the PV characteristic graph has the same number of peaks as the number of diodes in the panel. These maxima occur in regions with panel voltages of about 10, 23, and 36 volts, respectively.

4.2. BACKGROUND OF THE PROPOSED METHOD

The maxima of the power generated by the panel occur when the panel voltages are about 10, 23, or 36 volts at all shading patterns and irradiance levels, as demonstrated in the preceding section. In other words, there is always a maximum power point at these three voltages. Therefore, by checking the three voltage points, the MPPT algorithms can find the point that can give maximum power in partial shading conditions. However, these three points may vary depending on the panel type. Therefore, these three voltage points must be computed to apply the suggested technique to various panels.

The previous section shows that the difference between neighbor peak voltages is approximately equal to

$$\Delta V_x \cong \frac{V_{OC}}{number\ of\ the\ diodes} \tag{4.1}$$

When one of the local maximum power points is determined, equation 4.1 may be used to estimate the other two peaks. However, depending on the location of the LMPP, the panel voltage is changed by $\pm\Delta V_x$. Therefore, in Figure 4.4, the power-voltage characteristic of the panel is divided into three regions to find the position of LMPP.

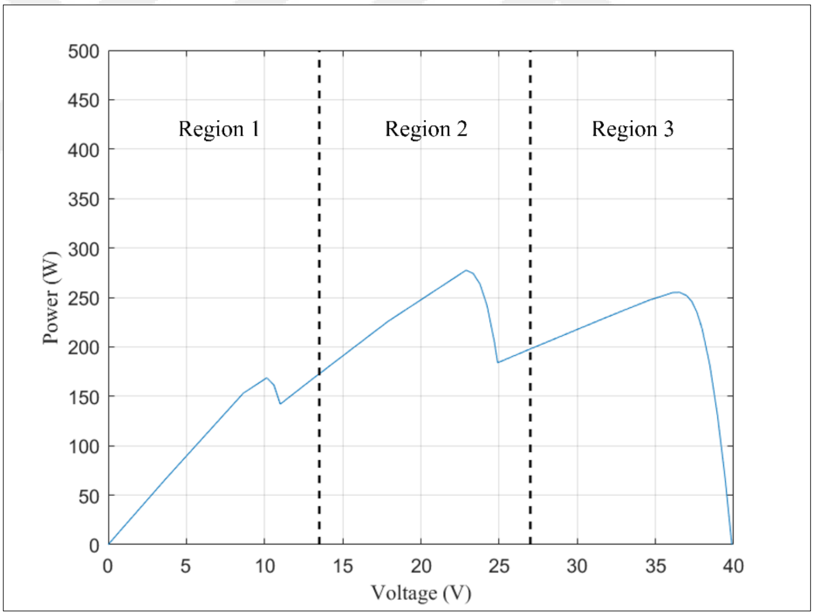

Figure 4.4. Regions of the P-V characteristics of the half-cut panel with three diodes

Each region can only have one peak, as shown in Figure 4.4. Thus, when the peak in a region is known, it may be estimated without measuring the approximate voltage value of the peaks of other regions.

4.3. PROPOSED METHOD

The proposed algorithm is based on the P&O algorithm. Under uniform radiation, the improved method utilizes the P&O approach to track the maximum power point. However, when partial shading is detected, the highest power value is selected by measuring the power values of the peaks. Figure 4.5 demonstrates the flowchart of the presented method.

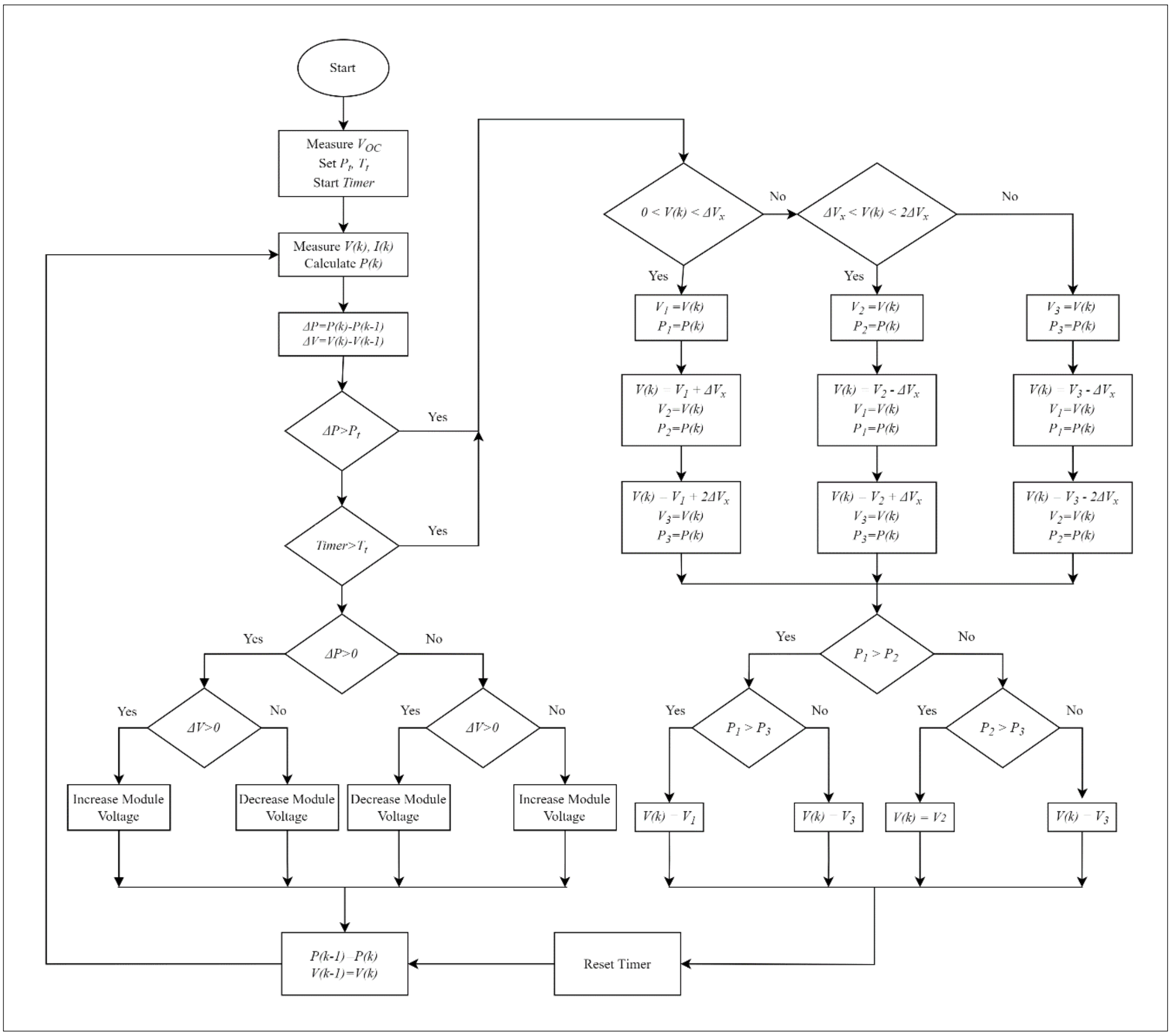

Figure 4.5. Flowchart of the proposed method

As seen in the flowchart, if the power difference value is less than a particular threshold value, the algorithm continues with the P&O algorithm. Thus, the P&O approach locates and tracks the initial peak. However, if the power change exceeds the limit value, the peak search technique is activated immediately. Also, if there is no power change for a certain period, the peak search algorithm is initialized in case of static shadowing. Then, the region is determined according to the last voltage value (V_{pv}) found by the P&O algorithm before the peak search algorithm starts.

Table 4.1. Voltage range of the regions

Region	**Voltage Range**
1	$0 < V_{pv} < V_{OC}/3$
2	$V_{OC}/3 < V_{pv} < 2V_{OC}/3$
3	$2V_{OC}/3 < V_{pv} < V_{OC}$

Table 4.1 shows the voltage ranges for each region. The voltage values corresponding to the possible LMPPs may vary depending on the region. Therefore, the voltages to be measured are obtained after defining the region depending on the voltage ranges. Table 4.2 lists the voltages of the possible LMPPs according to the regions.

Table 4.2. Voltage values of possible LMPPs by regions

Region	**The Voltages of**		
	First LMPP	**Second LMPP**	**Third LMPP**
1	V_{pv}	$V_{pv} + \Delta V_x$	$V_{pv} + 2\Delta V_x$
2	V_{pv}	$V_{pv} + \Delta V_x$	$V_{pv} - \Delta V_x$
3	V_{pv}	$V_{pv} - \Delta V_x$	$V_{pv} - 2\Delta V_x$

As seen in the table above, the voltage of the three potential LMPPs is determined. The power values corresponding to these three determined voltage values are measured and compared with each other. Consequently, the panel voltage is set to the voltage that produces the most power. Then, the conventional P&O algorithm starts from this voltage value and continues to track the maximum power point.

4.4. SIMULATION OF THE PROPOSED METHOD IN SIMULINK

MATLAB Simulink is utilized for the simulation and modeling of the proposed method. A 550-watt half-cut panel with three bypass diodes is modeled, and a boost converter is connected to the panel output in Simulink. There is also a function block to operate the converter and several blocks to monitor the data received from the system. Figure 4.6. demonstrates the Simulink modeling used in this study.

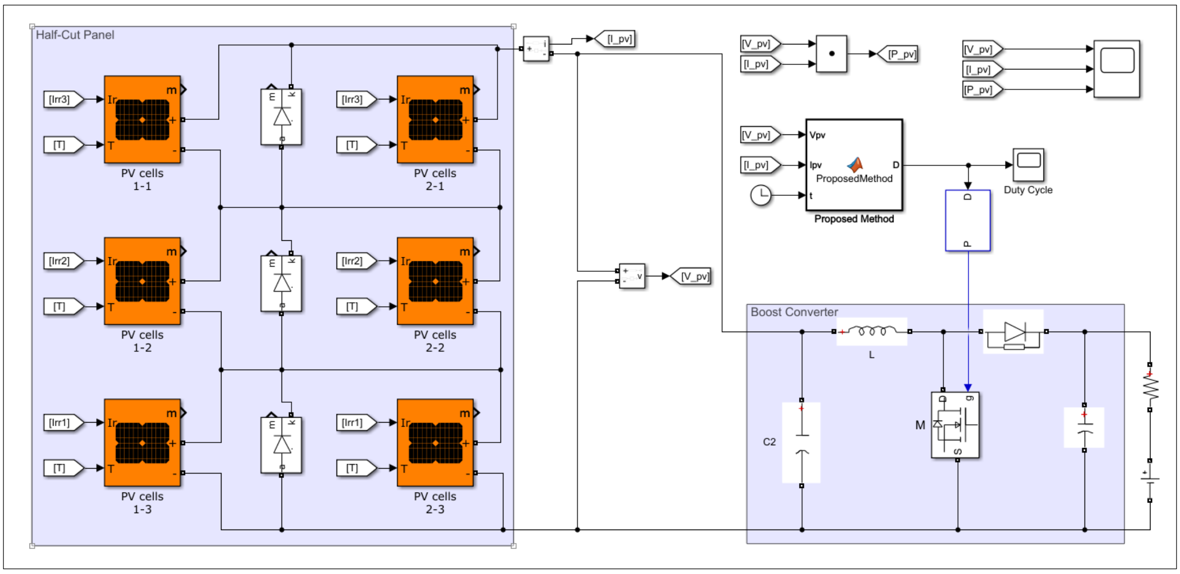

Figure 4.6. The Simulink model implemented in this study

The presented method is implemented to control the converter by adjusting the duty cycle. The calculation of the duty cycle for the boost converter is given in Equation 4.2.

$$D = 1 - \frac{V_{input}}{V_{output}} \tag{4.2}$$

Since the converter input is connected to the panel output, the duty cycle affects the panel voltage. The converter output voltage must be known to adjust the PV panel to a specific voltage, as deduced from the above equation. Therefore, the converter output voltage is fixed by adding a voltage source and a low-value resistor to the converter output. As a result, the desired panel voltage can be provided simply by adjusting the duty cycle.

The proposed method has been verified under various partial shading scenarios.

4.4.1. Static Partial Shading Simulation

The shadow on the panel does not vary over time when partial shading is static. Thus, since the panel characteristic will remain constant, the operating behavior of the proposed method may be easily analyzed in static partial shading conditions. A partial shading situation was created by applying 300-1000-700 w/m2 irradiation to three cell groups connected to the bypass diodes of the half-cut panel. In this circumstance, the P-V characteristic of the half-cut panel is shown in Figure 4.7.

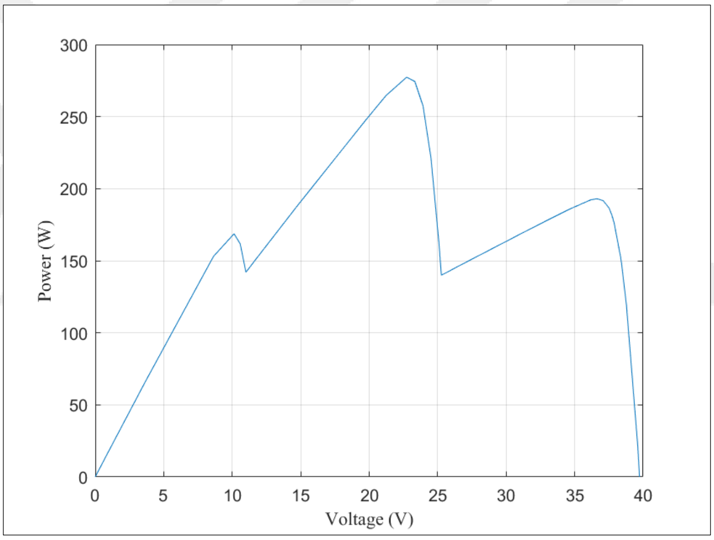

Figure 4.7. Power-Voltage characteristic of the half-cut panel

In Figure 4.7., when the panel voltage is 10-23-26 volts, there are LMPPs with a power of about 165-275-190 W, respectively. In these conditions, when the MPP is tracked with the conventional P&O approach, it will be stuck around 10 volts, which is the first peak, shown in Figure 4.8. As a result, only 165 watts will be produced instead of the maximum power that can be generated, which is 275 watts.

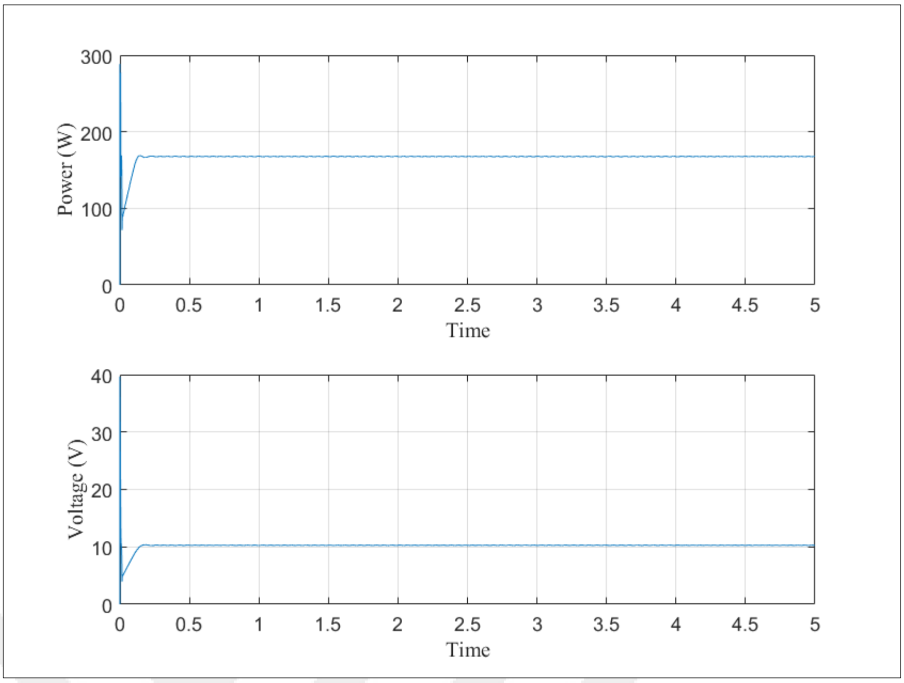

Figure 4.8. Power-Voltage graph of the panel when using P&O

The maximum power point was tracked using the presented technique instead of the P&O method. The peak search method in the proposed algorithm was activated in two and a half seconds. The values of three possible maximum power points, which are 10, 23 and 36 volts, are examined, and the power values corresponding to these voltages are compared, respectively. As a result, the voltage value corresponding to the highest power was selected. Then, the P&O algorithm was immediately engaged from this selected voltage to find the exact GMPP, as illustrated in Figure 4.9.

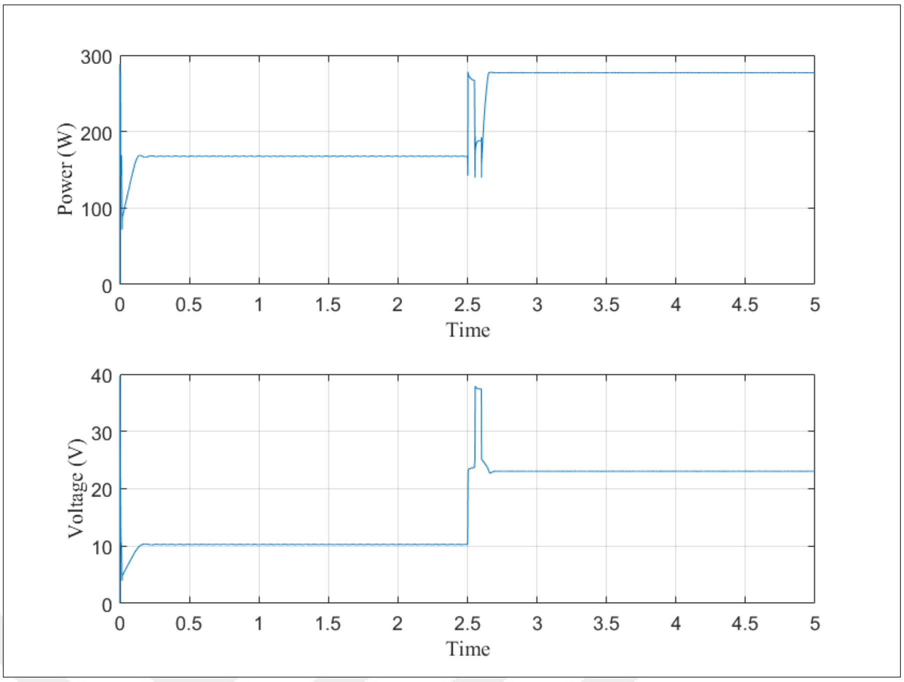

Figure 4.9. Power-Voltage graph of the panel when using the proposed method

4.4.2. Dynamic Partial Shading Simulation

The partial shading condition is caused by objects that cast a shadow on the part of the panel. Shading patterns and levels change throughout the day due to the movement of clouds or the change in the angle of sunlight. Therefore, environmental effects cannot be adequately represented by static partial shading. Thus, a dynamic partial shading pattern was created based on actual environmental conditions. Partial shading was simulated by applying variable radiation values to different parts of the PV panel. Figure 4.10. illustrates the amount of solar radiation received by the PV panel.

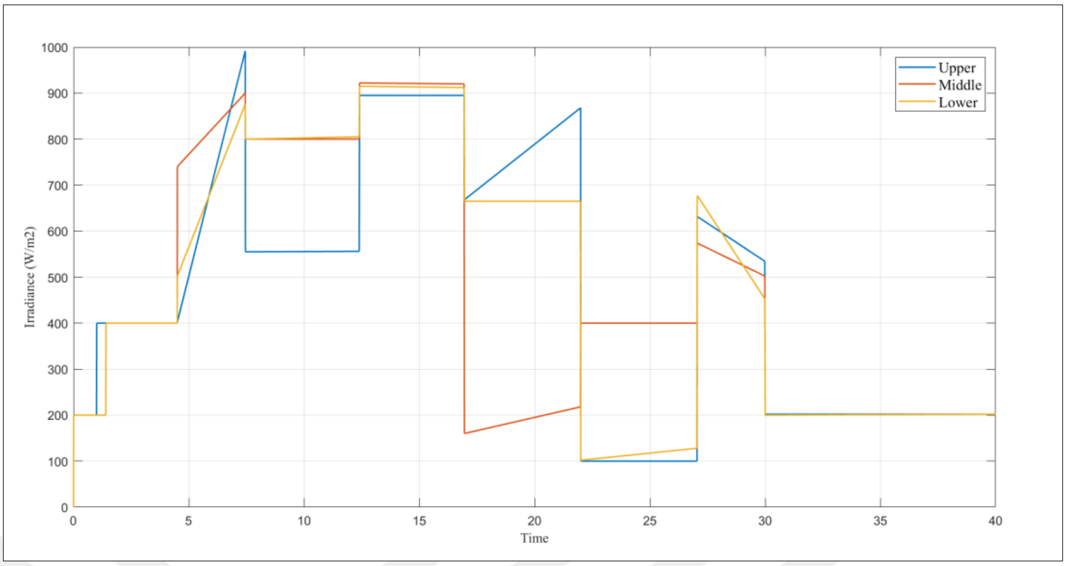

Figure 4.10. Irradiance levels according to the parts of the PV panel

The presented algorithm is simulated by applying the above irradiance pattern. The algorithm initiates the GMPP search in case of rapid power loss, on the contrary, it continues to follow the MPP with the P&O method when there is no power drop. Figure 4.11. demonstrates that the presented approach can track the ideal power graph by finding the GMPP in dynamic PSC.

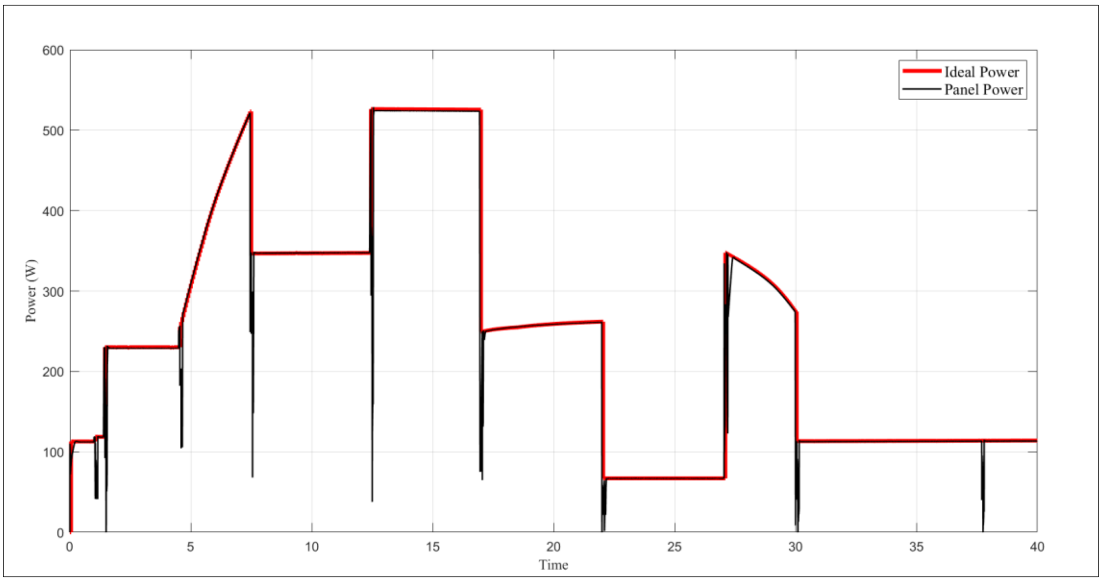

Figure 4.11. Ideal power vs. the panel power graph using the proposed algorithm

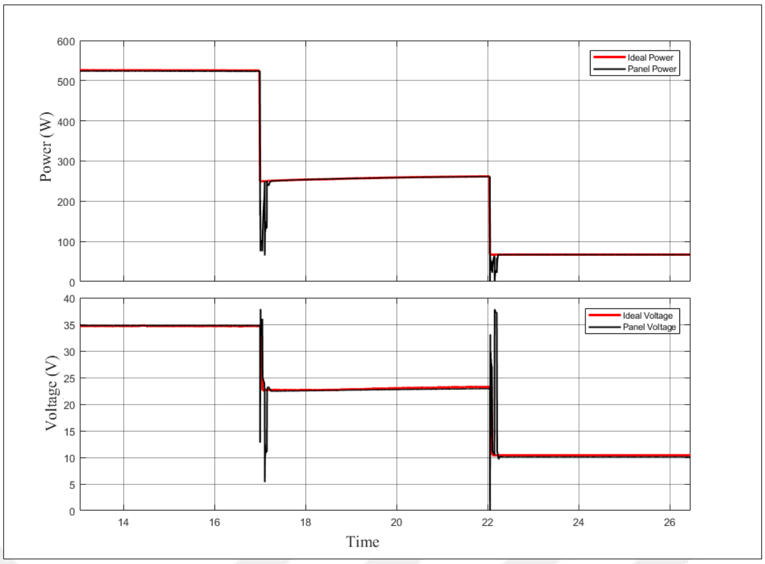

Figure 4.12. Comparison of P-V characteristics of ideal power and panel power

It is apparent from Figure 4.12, the voltage values that provide ideal power due to partial shading change as 35, 23 and 10 volts, respectively. The global search is activated when the power change is measured, and the panel voltage is adjusted to give ideal power, as seen in the figure above. Then, the optimal power was followed by tracking using the P&O algorithm.

4.5. IMPROVED PROPOSED METHOD

This proposed technique is designed for three bypass diode PV panel applications. Nonetheless, a novel approach has been devised to ensure that the proposed algorithm applies to all PV panels with diodes.

With the start of the peak search, the panel voltage ranges from zero to V_{OC} is divided into equal regions as the number of diodes (n). As a result, there is one possible power peak in each region. Thus, n power points are formed, denoted as $P_{1\dots n}$. After the regions are defined, using the final voltage value (V_{pv}) found by the P&O algorithm, the region (r) of the V_{pv} is calculated with the formula given in Equation 4.3.

$$r = \lceil V_{pv}/\Delta V_x \rceil \tag{4.3}$$

The voltage values corresponding to the possible LMPPs are calculated by changing the V_{pv} value in steps of $\pm\Delta V_x$. However, the number and direction of steps differ depending on the region of the V_{pv}. Table 4.3 provides the power and voltage values of the LMPPs to be formed according to diode numbers in the panel and the panel voltage.

Table 4.3. Power and voltage values of LMPP

Coefficient (k)	**Corresponding Power**	**Corresponding Voltage**
r	P_k	V_{pv}
1 to n	P_k	$V_{pv} + (\text{k} - \text{r})\Delta V_x$

Figure 4.13. illustrates the flowchart of the improved proposed algorithm regardless of the number of diodes in a panel.

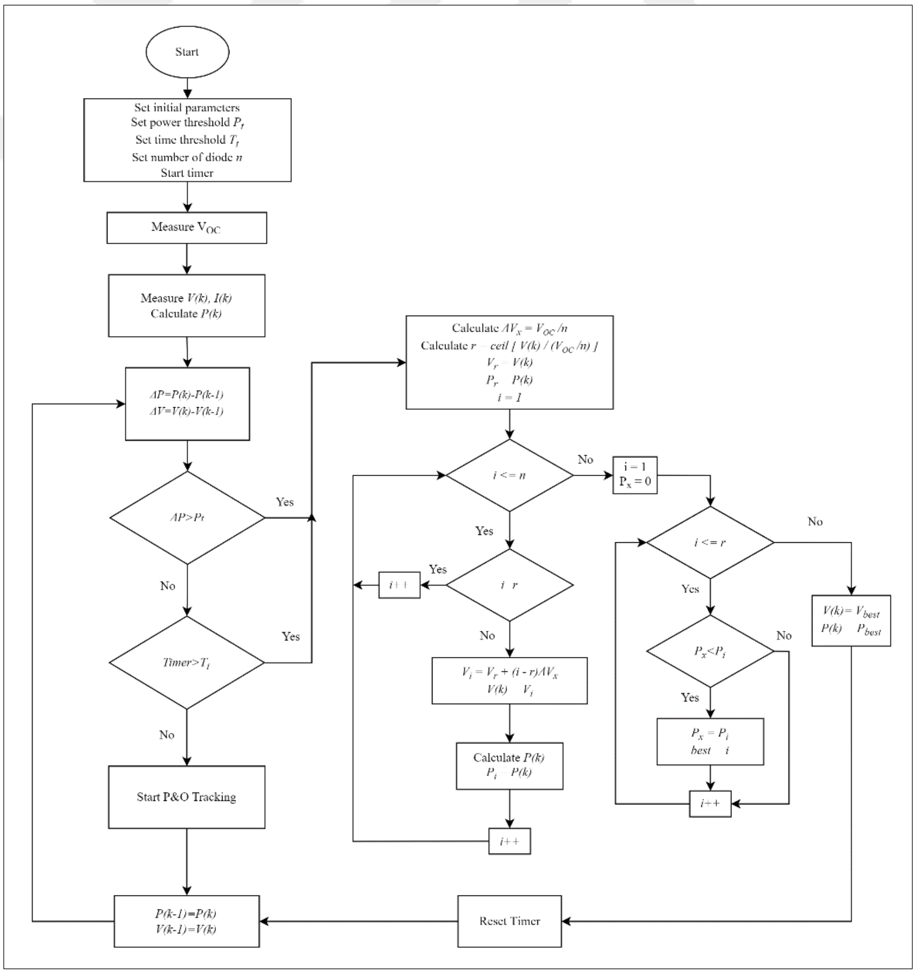

Figure 4.13. Flowchart of the improved proposed method

4.6. IDEAL POWER CALCULATION IN SIMULINK

Depending on the climatic factors, the voltage value corresponding to the maximum power generated by the PV panel changes. Therefore, the entire voltage range of the PV panel must be scanned to precisely determine maximum power. A block was designed to sweep the whole voltage range of the panel for each step size of the simulation. A controlled voltage source is connected to the PV panel output in order to adjust the panel voltage, as demonstrated in Figure 4.14. As a result, the ideal power that can occur in different environmental conditions and the corresponding voltage value are calculated instantly.

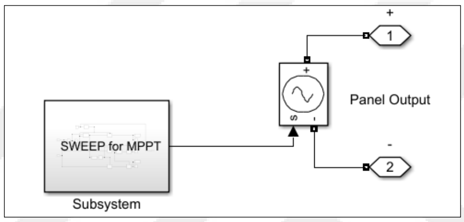

Figure 4.14. The control block of the panel voltage

The sweep to MPPT block continuously scans the voltage range of the panel by controlling the voltage source. As a result, the greatest power value for each step is determined, and the corresponding voltage value is recorded. Figure 4.15. shows the system of sweep to MPPT.

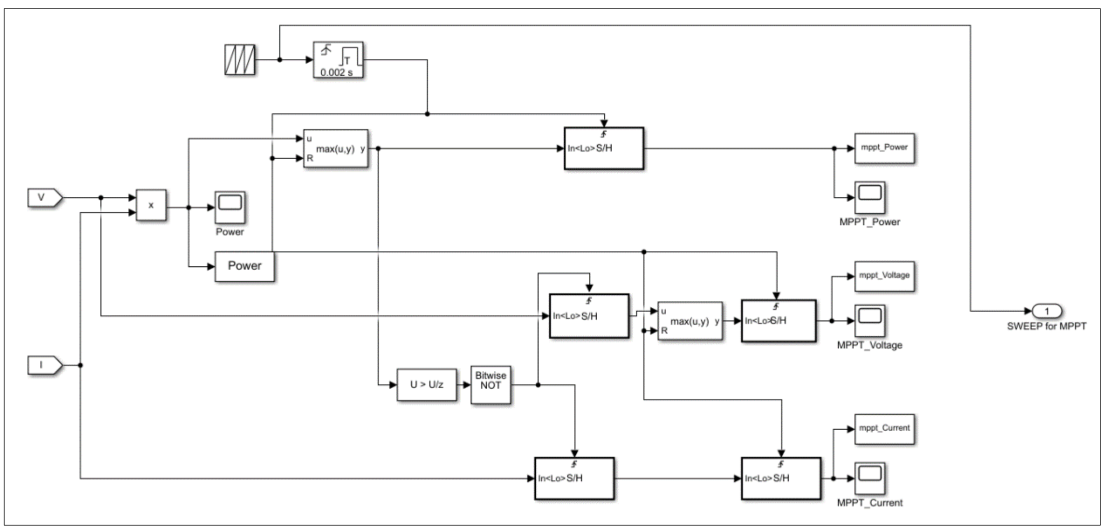

Figure 4.15. Subsystem of the voltage sweep

5. RESULTS AND DISCUSSION

MATLAB/Simulink software was used to assess and compare the suggested MPPT technique with existing algorithms. Since the presented algorithm is an alternative to random search algorithms, a hybrid simulated annealing (SA) and P&O algorithm in the literature was chosen for comparison. The hybrid approach that is being suggested combines the SA technique for continuous local searching with the P&O method for global searching. In addition, a global search is initiated if there is a significant change in power during the execution of the P&O method [44]. Except for the global search strategy, a hybrid SA and P&O algorithm is quite similar to the presented algorithm. While the hybrid algorithm conducts a random search to find the GMPP, the presented algorithm only examines the possible LMPP location, as mentioned in the previous section. The variable partial shading conditions presented in Figure 4.10 were applied to compare the performance of these algorithms.

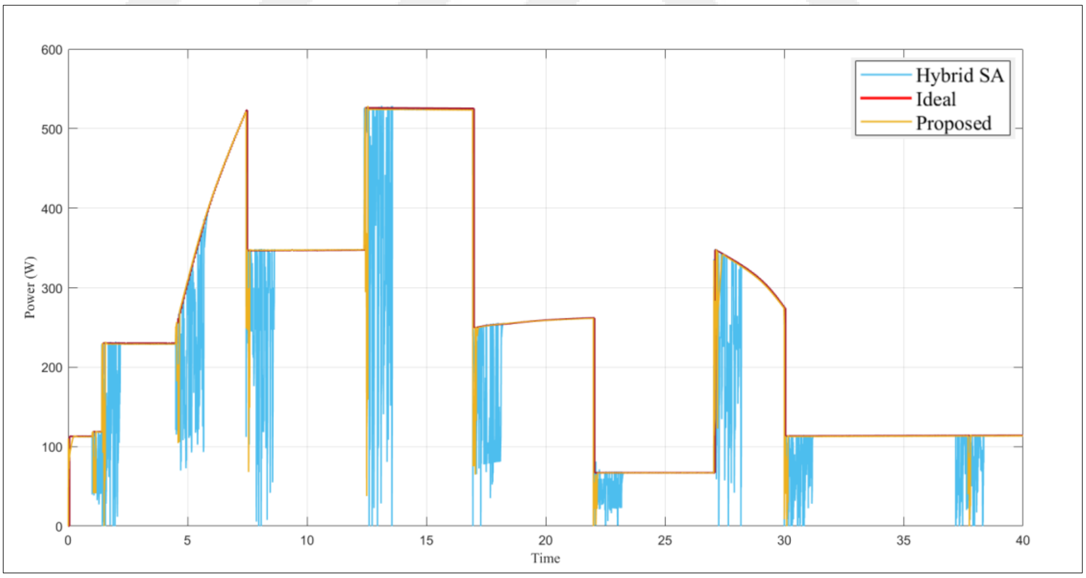

Figure 5.1. Comparison of P-V characteristics of the algorithms

As seen in the graph above, both methods effectively followed the ideal power graph. Table 5.1. shows the efficiency of the two algorithms according to the ideal power.

Table 5.1. Comparison of efficiency based on ideal power

Methods	Efficiency (%)
Proposed Algorithm	98.36
Hybrid Simulated Annealing	90.63

These results thus need to be interpreted with caution. These efficiency values vary depending on the irradiation levels, GMPP search frequency, simulation step size and time. Peak searching under high irradiance causes more power loss than low irradiance. Moreover, since the hybrid SA algorithm takes longer to search for GMPP, the efficiency gap between the proposed algorithm and the hybrid SA becomes more significant as the search mechanism engages. In addition, the SA parameters affect the global search time and peak finding accuracy. Since simulated annealing parameters studied in the literature are chosen for a wider voltage range, parameters that reduce the number of search steps are used in this study [43,45,46].

Apart from the complex partial shading analysis, the algorithm performance was also tested in clear weather conditions with few clouds. Moreover, irradiance levels are given randomly for more realistic analysis. Figure 5.2 shows the irradiance levels received by the different parts of the PV panel.

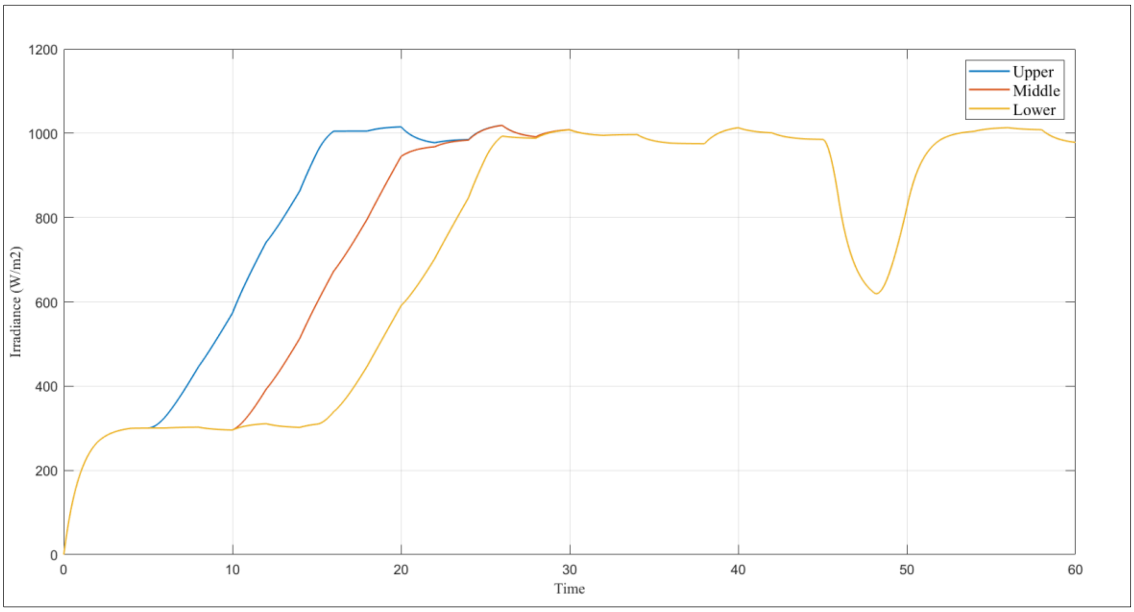

Figure 5.2. Irradiance levels according to the parts of the PV panel

The sunlight hits the PV panel from upper to lower at sunrise. In order to simulate this scenario, different irradiance levels are defined for the upper, middle, and lower parts of the PV panel, as seen in the graphic above. Furthermore, this simulation also includes the temperature changes caused by the sunlight hitting the panels.

Figure 5.2 demonstrates no sudden changes in irradiance, thus there will not be any significant differences in power either. The algorithms have been modified to consider the change in power that occurs in a certain period to initiate the general search. The proposed algorithm and hybrid SA are simulated according to the irradiance graph above, and the power and voltage comparison graph is indicated in Figure 5.3.

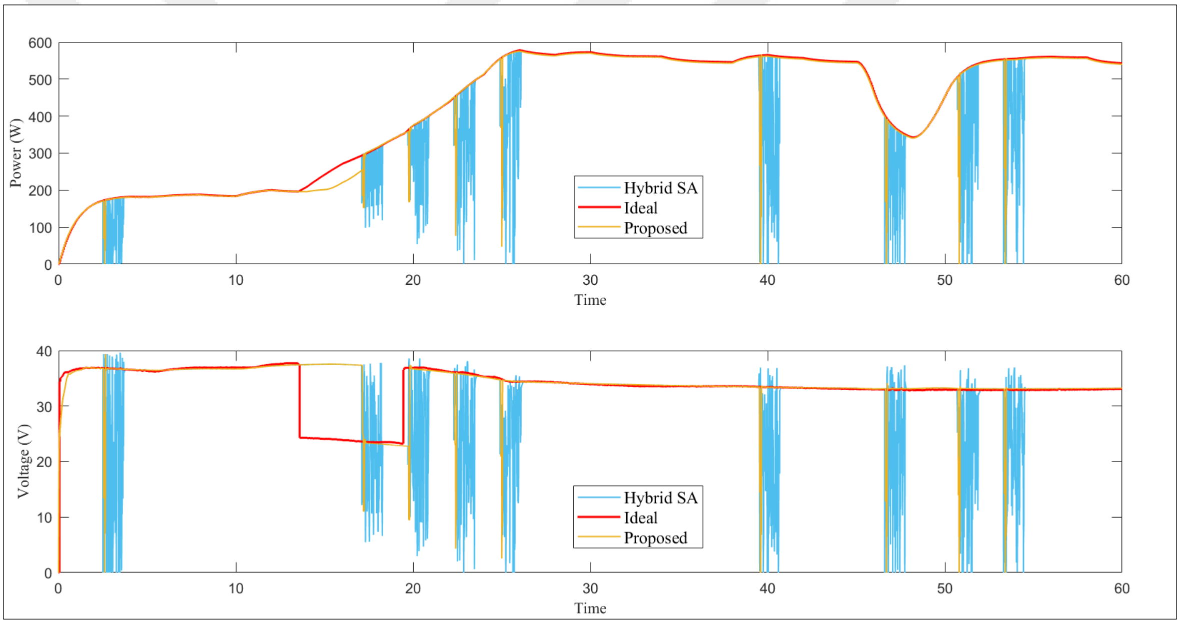

Figure 5.3. Comparison of P-V and I-V characteristics

The above graphs show that the algorithms cannot follow the peak in PSC at about 15th seconds. In addition, although the irradiance increases, the power of the PV panel remains constant. Because a new MPP is formed on the P-V characteristic due to partial shading, and the panel voltage remains at the LMPP point. However, after a particular time, the power increased, and the algorithms found the ideal power point by performing a global search. The efficiency results of the algorithms are presented in Table 5.2.

Table 5.2. Comparison of algorithms' efficiency

Methods	Efficiency (%)
Proposed Algorithm	98.38
Hybrid Simulated Annealing	93.53
Perturb and Observe	98.87

The results indicate that the presented method can produce more power compared to the hybrid SA. Not surprisingly, the conventional P&O approach was the most effective algorithm among the compared algorithms in conditions where uniform radiation dominates.

These results confirm that the presented algorithm works more efficiently than the hybrid SA algorithm in PSC. Besides efficiency, global search time is another critical factor in algorithm performance. A long search time is a disadvantage as it will cause incorrect selection in case of irradiance change. Hence, the proposed technique is in an advantageous position.

The analysis of the presented algorithm was done on a PV panel. However, several panels are connected in series in a solar power plant. As mentioned in the methodology, the panel's characteristic can contain as many LMPPs as the number of diodes. Hence, the number of LMMPs formed in a PV system equals the multiplication of the number of series connected panels by the diode number in one panel. However, in particular cases, the total number of the peaks depends on only the diode number in a panel regardless of the number of series connected panels.

The solar panels in the field solar power plant always block each other at sunrise and sunset. In this situation, the panels in series illuminate simultaneously with the same patterns. Therefore, series-connected PV panels, regardless of their number, have the characteristics of a single panel. Thus, only three LMPPs can occur like a single panel. The PVsyst software was used to simulate in order to demonstrate this shadowing. A field solar power plant was designed to illustrate this shading, and a shading analysis was performed using PVsyst software. The shading created by the panels in the power station is shown in Figure 5.4.

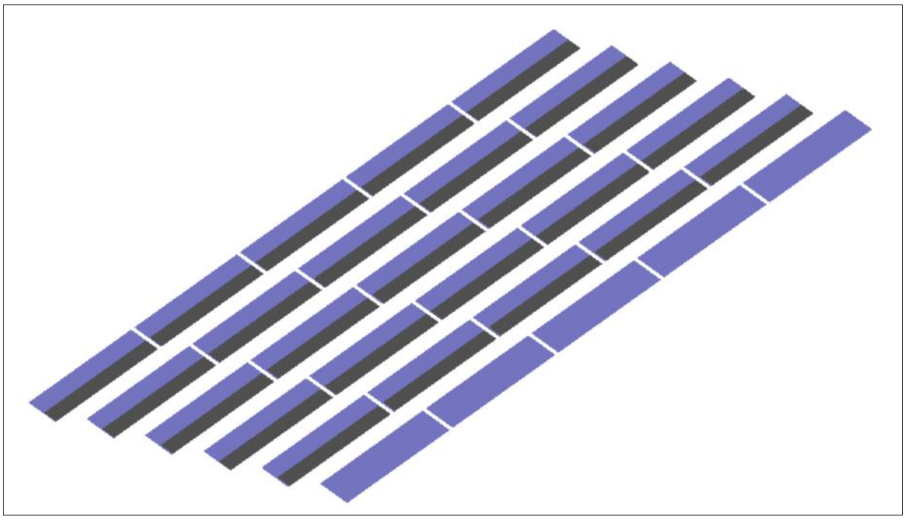

Figure 5.4. Shading analysis of the field solar power station

The time period in which this shading will occur can be predetermined according to the location of the power station. Power losses can be decreased by initiating global searching during these times.

6. CONCLUSION

This thesis proposes an effective MPPT algorithm for PV systems under partial shading conditions. MPPT algorithms must track the global power peak to extract the maximum power. However, multiple peak points appear on the P-V characteristic due to the effect of the bypass diode in case of partial shading. Furthermore, the locations of these peak points vary non-linearly with irradiance and temperature. Therefore, many algorithms struggle to detect GMPP in partial shading situations. This thesis presents a mechanism for determining the global peak by predicting potential maximum power points. The proposed algorithm first computes the possible maximum power points based on the open circuit voltage of the panel and the number of diodes, then measures the corresponding power of the points. After determining the GMPP, the proposed method continues to track utilizing the P&O approach. The presented technique was simulated at various irradiance patterns and temperatures using the Simulink software. The results of this study indicate that the proposed method performs more effectively than the Simulated Annealing algorithm in various environmental situations. The proposed and the Simulated Annealing algorithms were compared under two different environmental conditions depending on the dominance of uniform and non-uniform radiations. Under mostly uniform irradiance condition simulation, the proposed algorithm is more robust than the SA method, with about 98.38% and 93.53% efficiency rates, respectively. Similarly, depending on the simulation of non-uniform conditions, the presented method provides higher performance with 98.36% efficiency than SA, which yields 90.63% efficiency. The strong point of this thesis lies in providing a reasonable method for finding GMPP. As it measures specific power points, the proposed global searching mechanism does not cause excessive power loss. Furthermore, implementing the proposed technique is cost-friendly because it does not require an additional sensor or high computing power. However, there is a limitation due to partial shading detection. Since the global searching is initiated by detecting the power change in the PV system in the literature, the same technique has been applied in the proposed algorithm. Unfortunately, as a global search will be started at each power decrease, the algorithm performs unnecessary searches in uniform irradiance situations. Nevertheless, the proposed approach improves the efficiency of field power stations or PV applications. In addition, it is recommended that future studies should aim at enhancing the precise detection of partial shadowing.

REFERENCES

1. Kober T, Schiffer HW, Densing M, Panos E. Global energy perspectives to 2060 – WEC's World Energy Scenarios 2019. Energy Strategy Reviews. 2020 Sep 1;31.

2. Rabaia MKH, Abdelkareem MA, Sayed ET, Elsaid K, Chae KJ, Wilberforce T, et al. Environmental impacts of solar energy systems: A review. Science of the Total Environment. 2021 Feb 1;754.

3. Esram T, Chapman PL. Comparison of photovoltaic array maximum power point tracking techniques. IEEE Transactions on Energy Conversion. 2007 Jun;22(2):439–49.

4. Subudhi B, Pradhan R. A comparative study on maximum power point tracking techniques for photovoltaic power systems. IEEE Transactions on Sustainable Energy. 2013;4(1):89–98.

5. Femia N, Petrone G, Spagnuolo G, Vitelli M. Optimization of perturb and observe maximum power point tracking method. IEEE Transactions on Power Electronics. 2005 Jul;20(4):963–73.

6. Sera D, Mathe L, Kerekes T, Spataru SV, Teodorescu R. On the perturb-and-observe and incremental conductance mppt methods for PV systems. IEEE Journal of Photovoltaics. 2013;3(3):1070–8.

7. Lian KL, Jhang JH, Tian IS. A maximum power point tracking method based on perturb-and-observe combined with particle swarm optimization. IEEE Journal of Photovoltaics. 2014 Mar;4(2):626–33.

8. Zhang F, Thanapalan K, Procter A, Carr S, Maddy J. Adaptive hybrid maximum power point tracking method for a photovoltaic system. IEEE Transactions on Energy Conversion. 2013;28(2):353–60.

9. Yang Y, Zhao FP. Adaptive perturb and observe MPPT technique for grid-connected photovoltaic inverters. In: Procedia Engineering. 2011. p. 468–73.

10. Ahmed J, Salam Z. A Modified P and O Maximum Power Point Tracking Method with Reduced Steady-State Oscillation and Improved Tracking Efficiency. IEEE Transactions on Sustainable Energy. 2016 Oct 1;7(4):1506–15.

11. Kollimalla SK, Mishra MK. A novel adaptive p&o mppt algorithm considering sudden changes in the irradiance. IEEE Transactions on Energy Conversion. 2014;29(3):602–10.

12. Mohanty S, Subudhi B, Ray PK. A Grey Wolf-Assisted Perturb & Observe MPPT Algorithm for a PV System. IEEE Transactions on Energy Conversion. 2017 Mar 1;32(1):340–7.

13. Ahmed J, Salam Z. A Modified P and O Maximum Power Point Tracking Method with Reduced Steady-State Oscillation and Improved Tracking Efficiency. IEEE Transactions on Sustainable Energy. 2016 Oct 1;7(4):1506–15.

14. Ahmed J, Salam Z. An improved perturb and observe (P&O) maximum power point tracking (MPPT) algorithm for higher efficiency. Applied Energy. 2015 Jul 5;150:97–108.

15. Sera D, Kerekes T, Teodorescu R, Blaabjerg F. Improved MPPT method for rapidly changing environmental conditions. In: IEEE International Symposium on Industrial Electronics. 2006. p. 1420–5.

16. Kollimalla SK, Mishra MK. Variable perturbation size adaptive P&O MPPT algorithm for sudden changes in irradiance. IEEE Transactions on Sustainable Energy. 2014;5(3):718–28.

17. Aashoor FAO, Robinson FVP. A variable step size perturb and observe algorithm for photovoltaic maximum power point tracking. In: Proceedings of the Universities Power Engineering Conference. 2012.

18. Mohanty S, Subudhi B, Ray PK. A new MPPT design using grey Wolf optimization technique for photovoltaic system under partial shading conditions. IEEE Transactions on Sustainable Energy. 2016 Jan 1;7(1):181–8.

19. Bollipo RB, Mikkili S, Bonthagorla PK. Hybrid, optimal, intelligent and classical PV MPPT techniques: A review. Vol. 7, CSEE Journal of Power and Energy Systems. Institute of Electrical and Electronics Engineers Inc.; 2021. p. 9–33.

20. Beriber D, Talha A. MPPT techniques for PV systems. In: International Conference on Power Engineering, Energy and Electrical Drives. 2013. p. 1437–42.

21. Vinifa R, Kavitha A. Fuzzy based Maximum Power Point Tracking on a PV system. In: 2013 International Conference on Energy Efficient Technologies for Sustainability, ICEETS 2013. 2013. p. 329–33.

22. Ishaque K, Salam Z, Amjad M, Mekhilef S. An improved particle swarm optimization (PSO)-based MPPT for PV with reduced steady-state oscillation. IEEE Transactions on Power Electronics. 2012;27(8):3627–38.

23. Lyden S, Haque ME. A comprehensive study of the key parameters of the Simulated Annealing method for maximum power point tracking in photovoltaic systems. In: IEEE Power and Energy Society General Meeting. IEEE Computer Society; 2016.

24. Lee KY, Vlachogiannis JG. Optimization of power systems based on ant colony system algorithms: An overview. In: Proceedings of the 13th International Conference on Intelligent Systems Application to Power Systems, ISAP'05. 2005. p. 22–35.

25. Nie L, Mao M, Wan Y, Cui L, Zhou L, Zhang Q. Maximum power point tracking control based on modified abc algorithm for shaded PV system. In: 2019 AEIT International Conference of Electrical and Electronic Technologies for Automotive, AEIT AUTOMOTIVE 2019. Institute of Electrical and Electronics Engineers Inc.; 2019.

26. Sawant PT, Lbhattar PCT, Bhattar CL. Enhancement of PV system based on artificial bee colony algorithm under dynamic conditions. In: 2016 IEEE International Conference on Recent Trends in Electronics, Information and Communication Technology, RTEICT 2016 - Proceedings. Institute of Electrical and Electronics Engineers Inc.; 2017. p. 1251–5.

27. Nugraha DA, Lian KL, Suwarno S. A novel mppt method based on cuckoo search algorithm and golden section search algorithm for partially shaded pv system. Canadian Journal of Electrical and Computer Engineering. 2019 Jun 1;42(3):173–82.

28. Ahmed J, Salam Z. A soft computing MPPT for PV system based on Cuckoo Search algorithm. In: International Conference on Power Engineering, Energy and Electrical Drives. 2013. p. 558–62.

29. Sunny MSH, Ahmed ANR, Hasan MK. Design and simulation of maximum power point tracking of photovoltaic system using ANN. In: 2016 3rd International Conference on Electrical Engineering and Information and Communication Technology, iCEEiCT 2016. Institute of Electrical and Electronics Engineers Inc.; 2017.

30. Daraban S, Petreus D, Morel C. A novel global MPPT based on genetic algorithms for photovoltaic systems under the influence of partial shading. In: IECON Proceedings (Industrial Electronics Conference). 2013. p. 1490–5.

31. Chandrasekaran K, Sankar S, Banumalar K. Partial shading detection for PV arrays in a maximum power tracking system using the sine-cosine algorithm. Energy for Sustainable Development. 2020 Apr 1;55:105–21.

32. Ghasemi MA, Mohammadian Forushani H, Parniani M. Partial shading detection and smooth maximum power point tracking of PV arrays under PSC. IEEE Transactions on Power Electronics. 2016 Sep 1;31(9):6281–92.

33. Gosumbonggot J, Fujita G. Partial shading detection and global maximum power point tracking algorithm for photovoltaic with the variation of irradiation and temperature. Energies (Basel). 2019 Jan 9;12(2).

34. Villalva MG, Gazoli JR, Filho ER. Comprehensive approach to modeling and simulation of photovoltaic arrays. IEEE Transactions on Power Electronics. 2009;24(5):1198–208.

35. Hyeonah Park, Hyosung Kim. PV cell modeling on single-diode equivalent circuit. In: IECON 2013 - 39th Annual Conference of the IEEE Industrial Electronics Society. IEEE; 2013. p. 1845–9.

36. Suthar M, Singh GK, Saini RP. Comparison of mathematical models of photovoltaic (PV) module and effect of various parameters on its performance. In: 2013 International Conference on Energy Efficient Technologies for Sustainability. IEEE; 2013. p. 1354–9.

37. Mahmoud YA, Xiao W, Zeineldin HH. A parameterization approach for enhancing PV model accuracy. IEEE Transactions on Industrial Electronics. 2013;60(12):5708–16.

38. Femia N, Petrone G, Spagnuolo G, Vitelli M. Power electronics and control techniques for maximum energy harvesting in photovoltaic systems. CRC press; 2017.

39. Joshi A, Khan A, SP A. Comparison of half cut solar cells with standard solar cells. In: 2019 Advances in Science and Engineering Technology International Conferences (ASET). IEEE; 2019. p. 1–3.

40. de Soto W, Klein SA, Beckman WA. Improvement and validation of a model for photovoltaic array performance. Solar Energy. 2006;80(1):78–88.

41. Ross Jr RG, Smokler MI. Electricity from photovoltaic solar cells: Flat-Plate Solar Array Project final report. Volume VI: Engineering sciences and reliability. 1986;

42. Lian KL, Andrean V. A new MPPT method for partially shaded PV system by combining modified INC and simulated annealing algorithm. In: 2017 International Conference on High Voltage Engineering and Power Systems (ICHVEPS). IEEE; 2017. p. 388–93.

43. Lyden S, Haque ME. A Simulated Annealing Global Maximum Power Point Tracking Approach for PV Modules under Partial Shading Conditions. IEEE Transactions on Power Electronics. 2016 Jun 1;31(6):4171–81.

44. Lyden S, Haque ME. A hybrid simulated annealing and perturb and observe method for maximum power point tracking in PV systems under partial shading conditions.

In: 2015 Australasian Universities Power Engineering Conference: Challenges for Future Grids, AUPEC 2015. Institute of Electrical and Electronics Engineers Inc.; 2015.

45. Fan Y, Zhuo F, Yang Y, Wang F, Zhu T, Shi S, et al. An improved simulated annealing maximum power point tracking technique for PV array under partial shading conditions. In: 2016 18th European Conference on Power Electronics and Applications, EPE 2016 ECCE Europe. Institute of Electrical and Electronics Engineers Inc.; 2016.

46. Lyden S, Haque ME, Xiao D. Application of a Simulated Annealing technique for global maximum power point tracking of PV modules experiencing partial shading. In: IECON Proceedings (Industrial Electronics Conference). Institute of Electrical and Electronics Engineers Inc.; 2014. p. 1977–83.